Geoacoustic modeling of the sea floor

Edwin L. Hamilton

Naval Ocean Systems Center, San Diego, California 92152
(Received 17 December 1979; accepted for publication 13 August 1980)

Geoacoustic models of the sea floor are basic to underwater acoustics and to marine geological and geophysical studies of the earth's crust, including stratigraphy, sedimentology, geomorphology, structural and gravity studies, geologic history, and many others. A "geoacoustic model" is defined as a model of the real sea floor with emphasis on measured, extrapolated, and predicted values of those properties important in underwater acoustics and those aspects of geophysics involving sound transmission. In general, a geoacoustic model details the true thicknesses and properties of sediment and rock layers in the sea floor. A complete model includes water-mass data, a detailed bathymetric chart, and profiles of the sea floor (to obtain relief and slopes). At higher sound frequencies, the investigator may be interested in only the first few meters or tens of meters of sediments. At lower frequencies information must be provided on the whole sediment column and on properties of the underlying rocks. Complete geoacoustic models are especially important to the acoustician studying sound interactions with the sea floor in several critical aspects: they guide theoretical studies, help reconcile experiments at sea with theory, and aid in predicting the effects of the sea floor on sound propagation. The information required for a complete geoacoustic model should include the following for each sediment and rock layer. In some cases, the state-of-the-art allows only rough estimates, in others information may be nonexistent. (1) Identification of sediment and rock types at the sea floor and in the underlying layers. (2) True thicknesses and shapes of layers, and locations of significant reflectors (which may vary with sound frequencies). For the following properties, information is required in the surface of the sea floor, in the surface of the acoustic basement, and values of the property as a function of depth in the sea floor. (3) Compressional wave (sound) velocity. (4) Shear wave velocity. (5) Attenuation of compressional waves. (6) Attenuation of shear waves. (7) Density. (8) Additional elastic properties (e.g., dynamic rigidity and Lamé's constant); given compressional and shear wave velocities and density, these and other elastic properties can be computed. There is an almost infinite variety of geoacoustic models; consequently, the floor of the world's ocean cannot be defined by any single model or even a small number of models; therefore, it is important that acoustic and geophysical experiments at sea be supported by a particular model, or models, of the area. However, it is possible to use geological and geophysical judgement to extrapolate models over wider areas within geomorphic provinces. To extrapolate models requires water-mass data (such as from Nansen casts and velocimeter lowerings), good bathymetric charts, sediment and rock information from charts, cores, and the Deep Sea Drilling Project, echo-sounder profiles, reflection and refraction records (which show detailed and general layering and the location of the acoustic basement), sound velocities in the layers, and geological and geophysical judgement. Recent studies have provided much new information which, with older data, yield general values and restrictive parameters for many properties of marine sediments and rocks. These general values and parameters, and methods for their derivation, are the main subjects of this paper.

PACS numbers: 43.30.Bp, 92.10.Vz, 91.50.Ey, 43.40.Ph

INTRODUCTION

A "geoacoustic model" is defined as a model of the real sea floor with emphasis on measured, extrapolated, and predicted values of those properties important in underwater acoustics and those aspects of geophysics involving sound transmission. In general, a geoacoustic model details the true thicknesses and properties of sediment and rock layers in the sea floor. A complete model includes water-mass data, a detailed bathymetric chart, and profiles of the sea floor (to obtain relief and slopes).

Geoacoustic models of the sea floor are basic to underwater acoustics and to marine geological and geophysical studies of the earth's crust, including stratigraphy, sedimentology, geomorphology, structural and gravity studies, geologic history, and many others.

The role of the geologist–geophysicist involved in geoacoustic modeling is, first, to determine, with the users of the models, those properties of the sea floor which are required to support the terminal studies. The next step is to synthesize available data on these properties in useable forms. Because data are invariably insufficient, the modeler must also make measurements and conduct research in the fields of acoustically relevant properties of the sea floor. In these studies (unless specific models are required), emphasis should be on general cases so that reasonable predictions can be made in the absence of specific measurements. These predictions are usually based on extrapolations from similar areas and sediment types. The geoacoustic modeler can usually extrapolate the information in models within geomorphic provinces based on studies of structure, stratigraphy, sedimentology, and petrology of the sea floor.

At higher sound frequencies, the investigator may be interested in only the first few meters or tens of meters of sediments. At lower frequencies, information must be provided on the whole sediment column and on properties of the underlying rocks. Complete geoacoustic models are especially important to the acoustician studying sound interactions with the sea floor in several critical aspects: they guide theoretical studies, help reconcile experiments at sea with theory, and aid in predicting the effects of the sea floor on sound propagation.

The information required for a complete geoacoustic model should include the following for each sediment

 0001-4966/80/111313-28$00.80

and rock layer. In some cases, the state-of-the-art allows only rough estimates, in others, information may be nonexistent.

1. Identification of sediment and rock types at the sea floor and in the underlying layers.

2. True thicknesses and shapes of layers, and locations of significant reflectors (which may vary with sound frequencies).

3. Compressional wave (sound) velocities.
   a. Values in the surface of the sea floor and the ratio between sediment and bottom water velocities.
   b. Equations for sound velocity as a function of depth (from which gradients can be computed).
   c. Sound velocity in the surface of the acoustic basement.

4. Shear wave velocities.
   a. Values in the surface of the sea floor.
   b. Shear wave velocity as a function of depth.
   c. Shear wave velocity in the surface of the acoustic basement.

5. Attenuation of compressional waves.
   a. Values in the surface of the sea floor.
   b. Sound attenuation as a function of depth in the sea floor.
   c. Sound attenuation in the surface of the acoustic basement.

6. Attenuation of shear waves.
   a. Values in the surface of the sea floor.
   b. Shear wave attenuation as a function of depth in the sea floor.
   c. Shear wave attenuation in the surface of the acoustic basement.

7. Density.
   a. Values in the surface of the sea floor.
   b. Density as a function of depth in the sea floor.
   c. Density in the surface of the acoustic basement.

8. Additional elastic properties (e.g., dynamic rigidity and Lamé's constant); given compressional and shear wave velocities and density, these and other elastic properties can be computed.

There is an almost infinite variety of geoacoustic models; consequently, the floor of the world's ocean cannot be defined by any single model or even a small number of models. Therefore, it is important that acoustic and geophysical experiments at sea be supported by a particular model, or models, of the area. However, as noted above, it is possible to use geological and geophysical judgement to extrapolate models over wider areas within geomorphic provinces. To extrapolate models also requires water–mass data (such as from Nansen cast and velocimeter lowerings), good bathymetric charts, sediment and rock information from charts, cores, and the Deep Sea Drilling Project, echo-sounder profiles, reflection and refraction records (which show detailed and general layering and the location of the acoustic basement), and sound velocities in the layers.

The subject of geoacoustic modeling was reviewed in earlier reports (Hamilton).[1,2] Therefore, information in some of the following sections is repeated from these earlier reviews. However, later studies have provided additional, important information on compressional-wave velocity gradients, on velocity–density relations, on shear wave variations with depth, on density and porosity gradients, on the ratios of compressional and shear waves, and on the acoustic properties of calcareous sediments. The older data and newer information provide general values and restrictive parameters for many properties of marine sediments and rocks. These general values and parameters, and methods for their derivation are the main subjects of this paper. Additionally, some older figures are revised, and new measurements of sediment properties are presented in partially revised tables (Tables I and II). An example of a geoacoustic model is in Appendix A. In Appendix B is a selected, mathematical, viscoelastic model for marine sediments.

The methods used by the writer in the field and laboratory to acquire the necessary data for geoacoustic models have been described and discussed in previous reports (to be referenced in appropriate sections) and in the references in these reports. These reports also contain numerous references to the results of others, and no attempt is made herein to compile an exhaustive bibliography.

In the discussions which follow, frequent references will be made to the three general environments (Fig. 1): The continental terrace (shelf and slope), the abyssal hill environment, and the abyssal plain environment. These environments and associated sediments were discussed by Hamilton,[3] Menard,[4] and Shepard.[5] Each of these main environments usually has distinctive sediment types. In the continental terrace most of the sediments are from terrigenous sources and range from sands to silty clays. The deep-sea abyssal plains are usually covered with layers of silt-clays with thinner, intercalated layers of sands (in and near channels) and silt; these materials (turbidites) were carried along the bottom in turbidity currents and cover, smoothly, the originally rough topography. The abyssal hills are mostly covered by relatively thin layers of pelagic clay and siliceous oozes, with thicker deposits of calcareous ooze around the equator and on seamounts, plateaus, and islands where the sea floor is above the calcium carbonate compensation depth.

Sediment nomenclature on the continental terrace and in abyssal plains follows that of Shepard,[6] except that within the sand sizes, the various grades of sand follow the Wentworth scale. In the deep sea, pelagic clay contains less than 30% siliceous or calcareous material. Calcareous ooze contains more than 30% calcium carbonate, and siliceous ooze more than 30% silica in the form of Radiolaria or diatoms. The Shepard[6] size grades are shown in these deep-sea sediment types in order to show the effects of grain size on various properties.

The averaged results of the measurements and computations of acoustic and related properties of sediments at the Naval Ocean Systems Center (NOSC) to

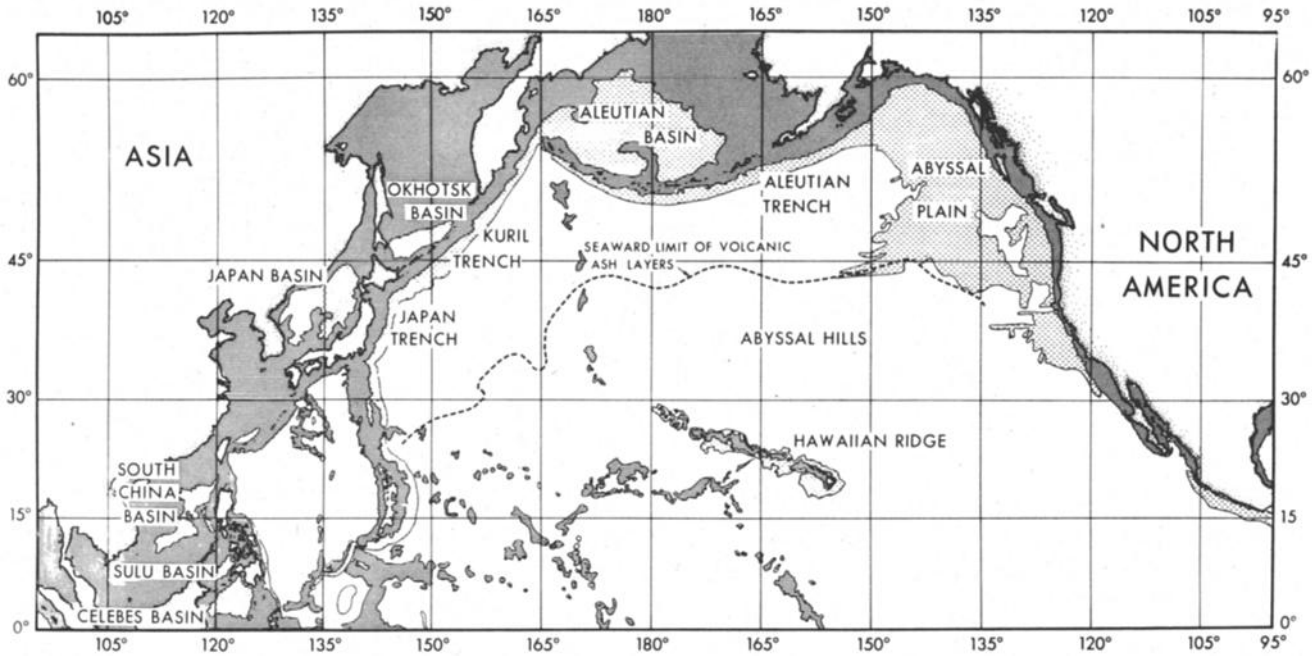

FIG. 1. Physiographic provinces and related environments, North Pacific and adjacent areas. See Hamilton[3] for references and discussion. The three general environments are continental terrace (shelf and slope): solid, horizontal lines; Abyssal plain (turbidite): horizontal, dashed lines; and abyssal hill (pelagic): white areas.

TABLE IA. Continental terrace (shelf and slope) environment; average sediment size analyses and bulk grain densities.

Sediment type	No. samples	Mean grain diam. (mm)	Mean grain diam. (ϕ)	Sand (%)	Silt (%)	Clay (%)	Bulk grain density (g/cm^3)
Sand							
Coarse	2	0.5285	0.92	100.0	0.0	0.0	2.710
Fine	22	0.1593	2.65	90.9	4.9	4.2	2.704
Very fine	12	0.0960	3.38	81.9	10.5	7.6	2.684
Silty sand	27	0.0490	4.35	57.6	28.9	13.5	2.689
Sandy silt	26	0.0308	5.02	28.0	59.2	12.8	2.680
Silt	19	0.0237	5.40	7.8	80.1	12.1	2.661
Sand–silt–clay	23	0.0172	5.86	32.3	41.6	26.1	2.701
Clayey silt	62	0.0077	7.02	7.3	60.0	32.7	2.660
Silty clay	19	0.0027	8.52	4.8	41.2	54.0	2.701

TABLE IB. Continental terrace (shelf and slope) environment; sediment densities, porosities, sound velocities, and velocity ratios.

	Density[a] (g/cm^3)		Porosity[a] (%)		Velocity[a] (m/s)		Velocity ratio[a]	
Sediment type	Av	SE	Av	SE	Av	SE	Av	SE
Sand								
Coarse	2.034	...	38.6	...	1836	...	1.201	...
Fine	1.941	0.023	45.6	1.02	1749	11	1.145	0.006
Very fine	1.856	0.022	50.0	0.97	1702	18	1.115	0.012
Silty sand	1.772	0.020	55.3	0.72	1646	10	1.078	0.006
Sandy silt	1.771	0.033	54.1	1.49	1652	12	1.080	0.007
Silt	1.740	0.047	56.3	1.30	1615	8	1.057	0.005
Sand–silt–clay	1.596	0.022	66.3	1.53	1579	8	1.033	0.005
Clayey silt	1.488	0.016	71.6	0.86	1549	4	1.014	0.003
Silty clay	1.421	0.015	75.9	0.82	1520	3	0.994	0.002

[a]Laboratory values: 23 °C, 1 atm; density: Saturated bulk density; porosity: Salt-free; velocity ratio: Velocity in sediment/velocity in sea water at 23 °C, 1 atm, and salinity of sediment pore water. SE: Standard error of the mean.

TABLE IIA. Abyssal plain and abyssal hill environments; average sediment size analyses and bulk grain densities.

Environment / Sediment type	No. samples	Mean grain diam. (mm)	Mean grain diam. (ϕ)	Sand (%)	Silt (%)	Clay (%)	Bulk grain density (g/cm^3)
Abyssal plain							
Clayey silt	24	0.0052	7.59	4.2	55.7	40.1	2.655
Silty clay	51	0.0021	8.87	3.0	35.3	61.7	2.665
Clay	6	0.0014	9.53	0.0	22.2	77.8	2.663
Bering Sea and Okhotsk Sea (siliceous-diatomaceous)							
Silt	1	0.0179	5.80	6.5	76.3	17.2	2.474
Clayey silt	5	0.0049	7.68	8.1	49.1	42.8	2.466
Silty clay	23	0.0024	8.71	3.0	37.4	59.6	2.454
Abyssal hill							
Deep-sea ("red") pelagic clay							
Clayey silt	17	0.0056	7.49	3.9	58.7	37.4	2.678
Silty clay	60	0.0023	8.76	2.1	32.2	65.7	2.717
Clay	45	0.0015	9.43	0.1	19.0	80.9	2.781
Calcareous pelagic sediment							
Sand-silt-clay [a]	193	0.015	6.1	...	...	...	2.683
Silt-clay [b]	166	0.006	7.3	...	...	...	2.656

[a] Includes sandy clay, clayey sand, silty sand, and sandy silt (coarser particles are mostly hollow Foraminifera).
[b] Includes clayey silt and silty clay (mostly finer calcareous particles).

TABLE IIB. Abyssal plain and abyssal hill environments; sediment densities, porosities, sound velocities, and velocity ratios.

Environment	Density [a] (g/cm^3)		Porosity [a] (%)		Velocity [a] (m/s)		Velocity ratio [a]	
Sediment type	Av	SE	Av	SE	Av	SE	Av	SE
Abyssal plain [b]								
Clayey silt	1.454	0.022	74.2	1.58	1528	3	0.999	0.002
Silty clay	1.348	0.014	80.5	0.98	1515	2	0.991	0.001
Clay	1.352	0.037	80.0	2.20	1503	2	0.983	0.001
Bering Sea and Okhotsk Sea (siliceous-diatomaceous)								
Silt	1.447	...	70.8	...	1546	...	1.011	...
Clayey silt	1.228	0.019	85.8	0.86	1534	2	1.003	0.001
Silty clay	1.214	0.008	86.8	0.43	1525	2	0.997	0.001
Abyssal hill								
Deep-sea ("red") pelagic clay								
Clayey silt	1.347	0.020	81.3	0.95	1522	3	0.995	0.002
Silty clay	1.344	0.011	81.2	0.60	1508	2	0.986	0.001
Clay	1.414	0.012	77.7	0.64	1493	1	0.976	0.001
Calcareous pelagic sediment								
Sand-silt-clay	1.435	0.007	75.3	0.38	1556	2	1.017	0.001
Silt-clay	1.404	0.011	76.9	0.64	1536	1	1.004	0.001

[a] Laboratory values: 23 °C, 1 atm pressure; density: Saturated bulk density; porosity: Salt free; velocity ratio: Velocity in sediment/velocity in sea water at 23 °C, 1 atm, and salinity of sediment pore water; SE: Standard error of the mean.
[b] For approximate properties of thinner, coarser-grained layers in abyssal plain turbidities: See continental terrace Tables IA and IB in the fine sand to sand-silt-clay sizes (silt is most common).

July 1979 are listed in Tables I and II. These data are for the upper 30 cm in the continental terrace where measurements were made *in situ* with probes, from diver-taken samples, and from cores. In deep-sea sediments, the upper 30 cm of gravity cores and deeper depths in piston cores furnished sediment for measurements. All velocity values are corrected to 23 °C and 1 atm pressure (Hamilton),[3] using tables for the speed of sound in sea water.

I. METHODS AND DISCUSSIONS

A. Introduction

In this section, the methods for deriving the various properties and components of a geoacoustic model will be discussed.

Before production of a geoacoustic model there are certain basic records and information which should or must be available either directly from an original survey or through published and unpublished literature and archival records in various institutions. These basic data and records are:

(1) Best-available bathymetric charts. If an expedition is involved, the ship's smoothed (corrected) track should be plotted on the chart with date–time notations along the tracks.

(2) Echo-sounder records; 12-kHz recorders on short pings, and/or 3.5-kHz recorders yield information on slope, relief, and reflectors in the upper tens of meters of the sea floor.

(3) Acoustic reflection profile records (such as air gun or electric-spark source) are absolutely essential to indicate major layering, reflectors, and acoustic basement, and to furnish sound travel time in the layers, from which true thicknesses of layers can be computed.

(4) Wide-angle reflection and refraction measurements (such as with expendable sonobuoys) of layer mean velocities and velocity gradients, and refraction velocities in the acoustic basement.

(5) Sediment samples from cores in which sound velocity, density, porosity, grain sizes, and other properties have been measured, and identification of sediment types determined; surface sediment charts are very useful.

(6) Oceanographic cast data (as from STD/SV or Nansen casts) to or near the sea floor, from which tables and curves of corrections from echo sounder to true depths, *in situ* sound velocity, temperature, salinity, pressure, and density versus true water depths can be determined.

(7) Literature information for the particular area on all aspects of the above, plus general geology of the area and region. The Initial Reports fo the Deep Sea Drilling Project are especially helpful.

B. Water-mass information

A necessary part of any geoacoustic model is information on the oceanic water layer overlying the sea floor. The required basic data are temperature, salinity, and sound speed as functions of true water depth. These data are ordinarily available from expeditions in the area or from computerized oceanographic archival information.

From the cast data, computations can be made of true depth versus pressure and density (Navoceano[7]). It is common practice to use Matthews' Tables (Navoceano,[7] p. 63) for corrections of echo sounder to true depths when specific information in an area is not available. It is important that all echo-sounder water depths in the model be corrected to true depths. The bottom-water temperature, salinity, sound speed, pressure, and density can be extrapolated to true depth of the sea floor at the location of the model. These values, plus computed impedance are placed in a table of bottom water properties which forms part of the geoacoustic model.

C. Bathymetric charts, ship's tracks, and profiles of the sea floor

The best available bathymetric charts of the area being modeled are an important part of geoacoustic modeling. Such charts can ordinarily be obtained from the Defense Mapping Agency, from Navoceano, from the literature, and/or from unpublished institutional information.

When modeling in support of an acoustic expedition, it is important that the smoothed (corrected) tracks of the expedition ships be plotted on the bathymetric charts with date–time notations along the tracks. Soundings from the echo-sounder records can then be annotated along the ship's tracks and the underlying water-depth contours can be corrected. The final results form a best chart of bottom topography. Such charts, with acoustic reflection profiler records, are essential elements in extrapolating models within geomorphic provinces. Additionally, the corrected navigational plots are critical to the underwater acousticians in determining the true geometry of experiments. And the corrected topographic charts allow studies of possible interactions of sound with the sea floor.

Another important part of a geoacoustic model are profiles of the sea floor along insonified tracks. These are usually derived from the echo-sounder records and the bathymetric chart. Such profiles yield evidence on bottom relief and slope.

D. Sediment surface properties

The properties of the surface of the sea floor are required in geoacoustic modeling. These properties can best be determined from *in situ* measurements accompanied by coring (e.g., Tucholke and Shirley[8]), or from laboratory measurements in cores, corrected to *in situ* values.[1-3,9,10]

In the absence of *in situ* measurements or cores from an area, values of necessary properties can be predicted from tables such as those in this report (Tables I, II). Proper use of the tables requires preliminary prediction of environment and sediment type, and final correction of tabulated values to *in situ* values using

methods discussed in detail by Hamilton.[1-3] Since these reports were published, additional information is available on velocity gradients, shear wave velocity and attenuation, density versus depth in the sea floor, and other information (as discussed in following sections).

E. Compressional wave (sound) velocity

There are two important elements in derivation of a curve and equations for compressional wave velocity (hereafter called sound velocity or velocity) versus depth in the sea floor: (1) a value of velocity at the sediment surface (designated as V_0), and (2) the variations of velocity with depth in the sea floor.

The value of sound velocity at the sediment surface can be predicted from tables or corrected to *in situ* from laboratory measurements in core samples.[3] These corrections can be made by full corrections from laboratory to *in situ* pressures and temperatures from tables for the speed of sound in sea water,[7] or more easily, by multiplying the velocity in the bottom water (from cast data) by the velocity ratio: sediment velocity in the laboratory at a certain temperature divided by sound speed in sea water at one atmospheric pressure and the same temperature; salinity is assumed to be the same in the sediment pore water as in the bottom water. This ratio remains the same in laboratory or *in situ* at various water depths; a separate column in Tables I and II list averaged values of the velocity ratio in various sediment types.

In constructing curves of velocity versus depth or time using sonobuoy data, an immediate problem concerns the velocity value for the sediment surface, V_0. This problem occurs because the first interval velocity from sonobuoy data is at the midpoint of the first layer. These values are usually 50–100 m or more below the water–sediment interface.

To determine a reasonable velocity gradient in the top of the sediment column it is essential to measure or predict velocity in the surface of the sea floor. Additionally, when regression equations are computed for velocity versus depth or travel time, it is essential that the curves be forced through these surface velocities (as done by Houtz *et al.*,[11,12] and by Hamilton *et al.*[13,14]). Otherwise, the intercept of the regression curves at travel time, $t=0$ (sediment surface velocity), and the upper velocity gradient are statistical artifacts (Houtz,[15] Hamilton *et al.*[13,14]). This is apt to be especially true when a first order, linear equation is used and higher velocity, lower, rock layers are included with the first layer data.

At present there are two main techniques for determining layer interval velocities in the sea floor. These are the sonobuoy method (as developed largely by Clay and Rona[16]; LePichon *et al.*[17]; Houtz *et al.*[11]; and Knott and Hoskins,[18] and the more recent technique using multichannel, continuous reflection profiling with very long hydrophone arrays and special processing of tape-recorded signals (e.g., Schlee *et al.*[19]; Taner and Koehler.[20] Both methods, however, yield no velocity information in the top of the first sediment layer which is of critical interest in modeling the sea floor for underwater acoustics.

A recent paper (Hamilton[21]) established velocity gradients in the top parts of the first sediment layers by fixing the sonobuoy regression equations to an independently derived, sediment surface velocity, V_0. The values of V_0 were derived from velocity measurements in cores as previously described. It is important therefore to independently confirm these upper sediment velocity gradients and values of V_0 by *in situ* measurements. *In situ* values of V_0 as measured by scuba divers, from submersibles, and by wide-angle reflection techniques are very close (within one percent) to measurements in cores corrected to *in situ* values (Houtz and Ewing[22]; Hamilton[3,9,23]; Fry and Raitt[24]), but until recently, no direct *in situ* measurements of velocity gradients had been published for the deep-sea floor.

Tucholke and Shirley[8] reported six *in situ* measurements of V_0 and velocity gradients to about 12 m in pelagic sediments and in turbidites in the North Atlantic. They used a velocimeter attached to a piston corer. The measured velocity gradients ranged from 0.5 to 1.1 s^{-1}. These values are within the maximum range reported herein for sonobuoy data. Sound velocity ratios (velocity in sediment/velocity in bottom water) reported by Shirley averaged 0.983 in pelagic clay and 0.990 in turbidites. These velocity ratios were within about one percent of those measured by Tucholke in the cores taken at the time of the velocimeter measurements. The velocity ratios reported by Shirley are almost exactly those reported by Hamilton[10] (p. 298) in these sediment types: 0.984 in pelagic clay (122 samples of clayey silt, silty clay, and clay) and 0.993 in turbidites (68 samples of clayey silt, silty clay, and clay).

An example of regional velocity-versus-travel time curves are those for the Bengal Fan (Hamilton *et al.*[14]) in the Indian Ocean (Fig. 2). The interval velocities were determined by analyses of wide-angle reflection (sonobuoy) data following LePichon *et al.*,[17] Houtz *et al.*,[11] and Houtz.[15] This method was outlined by Hamilton *et al.*[13,14] When these interval velocities are regionally grouped and plotted versus one-way sound travel time from the sediment surface to the interval velocity point (midpoint in time of the layer), the regression on these data furnishes an equation of instantaneous velocity, V, versus one-way travel time. Equations for mean velocity, $\bar{V}$, versus travel time, and instantaneous velocity versus depth can be derived from the same data.

In a recent report (Hamilton[21]) sonobuoy data were assembled for 20 areas in upper, unlithified layers of mostly turbidite sections in various oceans. Instantaneous velocity, and mean velocity versus one-way travel time (Fig. 3), and instantaneous velocity versus depth diagrams (Fig. 4) illustrate the results. In these diagrams, the regression curves were forced through an average surface-sediment value of 1511 m/s, based on measurements in cores corrected to *in situ* values. The error bars represent the 95% confidence limits on these data. That part of the velocity versus time and depth curve (Figs. 3, 4) from about 750–1000 m was

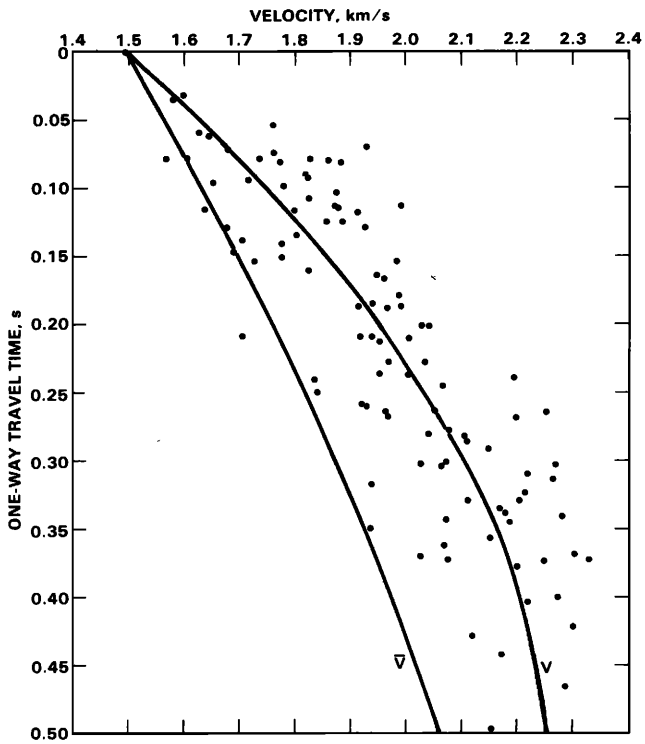

FIG. 2. Instantaneous compressional wave (sound) velocity V, and mean velocity, $\bar{V}$, versus one-way travel time of sound in the central Bengal Fan. See Hamilton *et al.*[14] for discussions and regression equations.

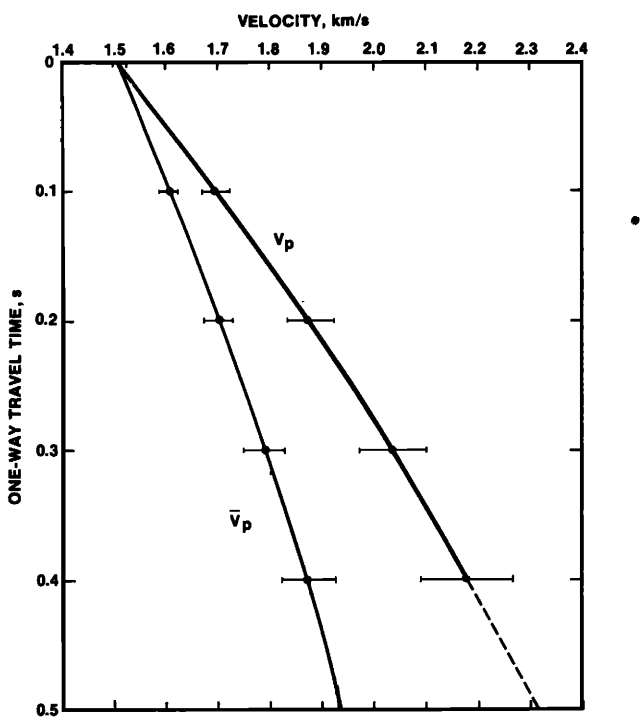

FIG. 3. Instantaneous compressional wave velocity, V_p, and mean velocity, $\bar{V}_p$, versus one-way travel time of sound in the sea floor in 20 areas of terrigenous sediments (silt-clays, turbidites, mudstone, shale). The data from 20 areas were averaged at increments of 0.1 s. The horizontal bars represent the 95% confidence limits. See Table III for regression equations.

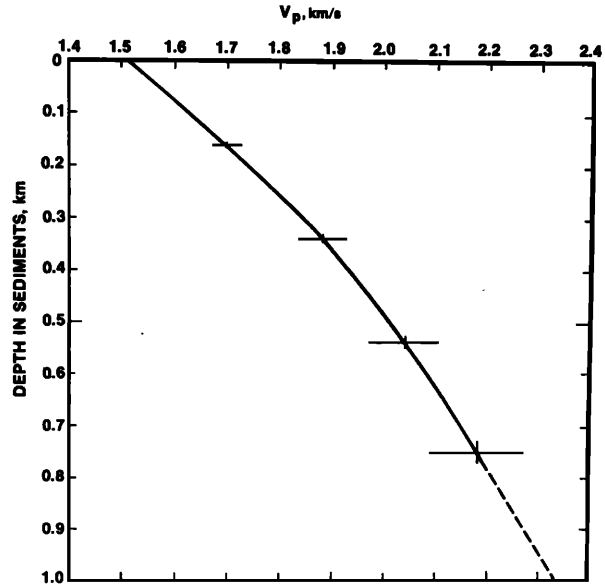

FIG. 4. Instantaneous compressional wave (sound) velocity versus depth in the sea floor in 20 areas of terrigenous sediments (silt-clays, turbidites, mudstone, shale). The error bars represent the 95% confidence limits. See Table IV for regression equation.

extrapolated in extension of the data, but also parallel or subparallel to velocity–depth functions within these depths from Houtz[15] (Atlantic Abyssal Plain, Bay of Bengal), Perrier and Quiblier[25] (shale), Magara[26] (mudstone), and Naini and Talwani[27] (abyssal fan in the Arabian Sea).

Velocity versus time and depth functions (Fig. 5) were derived for a thick calcareous section including calcareous ooze, chalk, and limestone from the Ontong–Java Plateau, and in siliceous sediments of the Bering Sea. The regression equations for these various sediment and underlying rock types are in Tables III, IV, and V.

Lacking sonobuoy measurements in an area of turbidites, one way to predict velocity versus time and depth functions for a geoacoustic model would be to use the 20-area information and equations (Figs. 3, 4; Tables III, IV, V) with an appropriate, predicted V_0 (substituted for the first coefficient in the equations). Equations could also be computed using the 20-area gradient equation (next section) plus the predicted V_0, and assumed one-way sound travel times. This latter method was used by White and Klitgord[28] to compare their data in the Gulf of Oman with data from Hamilton *et al.*,[13] for 13 areas of terrigenous sediments; the results were good (Fig. 6). Similar predictions for calcareous and siliceous sediments could be made by using the data in Hamilton.[21]

In shallow water, or in and near turbidity-current channels in abyssal plains, sands can form important deposits.

Hamilton[29,30] illustrated data from the Shell Development Company relating laboratory measurements of compressional and shear wave velocities to pressure in brine-saturated fine and coarse sands. In the 1976

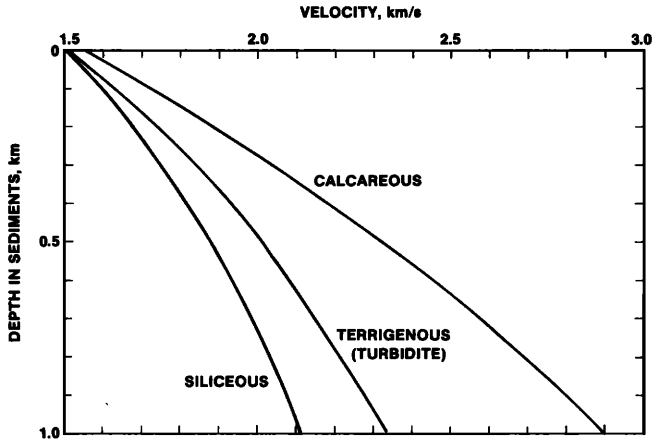

FIG. 5. Instantaneous compressional wave (sound) velocity versus depth in the sea floor for three principal sediment types. The "Siliceous" curve represents diatomaceous sediments in the central Bering Sea. The "Terrigenous" curve represents the 20 areas of terrigenous sediments illustrated in Fig. 4. The "Calcareous" curve represents calcareous ooze, chalk, and limestone from the Ontong–Java Plateau in the western equatorial Pacific. See Table IV for regression equations

report the pressure data were converted to depths in the sands and it was recommended that compressional wave velocity, V (in m/s) versus depth, D (in m) be predicted using $V = KD^{0.015}$; where K is a constant.

In order to study velocity gradients in sand, the following procedure was used to compute an example. (1) A value of 1.147 for the velocity ratio (sediment/sea water) in fine sand was taken from laboratory measurements (Hamilton,[10] Table A-1a). (2) This ratio was used to get an *in situ*, sediment-surface velocity at 20-m water depth off San Diego: V_0 = velocity ratio × velocity in bottom water = 1.147 × 1506 = 1727 m/s. This velocity was assumed to be at a depth in the sand of 5 cm (half the thickness of a typical laboratory sample). (3) The values of velocity (1727 m/s) and depth (0.05 m) were entered into the above equation which was solved for the constant K (1806 m/s). The equation was used in the computations was then: $V = 1806D^{0.015}$. Velocities to a depth of 20 m in fine sand were then computed (Fig. 7).

TABLE III. Coefficients of regression equations. Instantaneous velocity V, and mean velocity $\bar{V}$, in km/s, as a function of one-way travel time t, in seconds, in the form: V or $\bar{V} = A + Bt + Ct^2$.

Sediment type; area	Velocity	A	B	C	SE[a]
Terrigenous sediments (silt clays, turbidites, mudstone shale); av 20 areas					
	V	1.511	1.983	−0.758	···
	$\bar{V}$	1.511	1.041	−0.372	···
Diatomaceous silty clay; Bering Sea					
	V	1.509	1.414	−0.574	0.113
	$\bar{V}$	1.509	0.707	−0.191	···
Calcareous ooze, chalk, limestone; Ontong–Java Plateau					
	V	1.559	2.965		0.080
	$\bar{V}$	1.559	1.487		0.054

[a]Standard error of estimate, km/s.

TABLE IV. Coefficients of regression equations. Instantaneous velocity V, in km/s, as a function of depth in the sediments Z, in km, in the form: $V = A + BZ + CZ^2 + DZ^3$.

Sediment type; area	A	B	C	D
Terrigenous sediments (silt clays, turbidites, mudstone shale); av. 20 areas	1.511	1.304	−0.741	0.257
Diatomaceous silty clay; Bering Sea	1.509	0.869	−0.267	
Calcareous ooze, chalk, limestone; Ontong–Java Plateau	1.559	1.713	−0.374	
Fine sand	(See footnote a)			

[a]Velocity, V, in m/s as a function of depth, Z, in m, for fine sand (in the depth interval of 0–20 m): $V = 1806Z^{0.015}$; see Hamilton[30] and text for discussion.

A complete geoacoustic model may include velocities in sedimentary rocks, and always, velocity in the surface of the acoustic basement. Mean, or layer interval, velocities in mudstone, shale, and limestone are frequently computed from sonobuoy reflection records. In many cases there are refraction returns represented in the sonobuoy records. Refraction velocities are usual in the literature of seismic exploration. A refraction yields the velocity in the top of a layer.

Given a refraction velocity in the top of a layer above the acoustic basement, it is necessary to compute mean velocity, the velocity at the bottom of the layer, and layer thickness. These velocities and thicknesses can be computed by (1) considering the refraction velocity as V_0, (2) measuring one-way sound travel time from the reflection records, (3) assuming the velocity gradient, $\bar{a}$, is linear and the same as in thick sections of similar rock at equivalent depths. For example, as illustrated in the lower parts of the diagrams for terrigenous sediments, mudstone, shale (Fig. 4), or calcareous ooze, chalk, limestone (Fig. 5), or from other data such as in Houtz,[15] and (4) using the equation: thickness, $h = V_0(e^{\bar{a}t} - 1)/\bar{a}$. After the thickness has been computed, the velocity at any given level can be computed with: $V = V_0 + \bar{a}h$.

TABLE V. Equations for mean velocity gradients, $\bar{a}$, in s^{-1}, between the sediment surface and any given one-way travel time, t, in s, for some principal sediment types.

Terrigenous sediments (silt clays, turbidites, mudstone shale); av. 20 areas	$\bar{a} = 1.284 - 0.963t - 0.897t^2 + 2.306t^3$
Diatomaceous silty clay; Bering Sea	$\bar{a} = 0.937 - 0.802t + 0.348t^2$
Calcareous ooze, chalk, limestone; Ontong–Java Plateau	$\bar{a} = 1.902 - 1.710t + 0.972t^2$

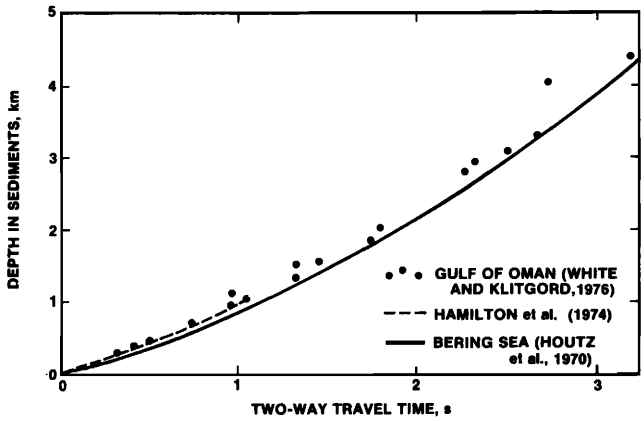

FIG. 6. Two-way sound travel time (reflection time) versus depth in the sea floor in the Gulf of Oman where the sediments are mostly turbidites (after White and Klitgord[28]). The round dots represent sonobuoy measurements. The dashed line represents predictions by White and Klitgord based on a sediment surface velocity and averaged values of velocity gradients in 13 areas of mostly turbidites (from Hamilton *et al.*[13]). The solid curve represents thick Bering-Sea sediments from Houtz *et al.*[12]

A velocity in the surface of the acoustic basement (frequently basalt) can usually be found from sonobuoy or explosive seismic refraction measurements in the literature for the general area. The Initial Reports of the Deep Sea Drilling Project are a fruitful source for such information.

If the mean velocity, $\overline{V}$, has been measured in a rock layer (such as by the sonobuoy technique), the true thickness can be computed by $h = \overline{V}t$. Velocities at the bottom and top of the layer can then be computed by assuming a velocity gradient, as above, and with the equation: Velocity at bottom or top $= \overline{V} \pm \overline{a}h/2$.

F. Compressional wave velocity gradients

A recent paper (Hamilton[21]) summarized sound velocity gradients in marine sediments. The following information is from that report.

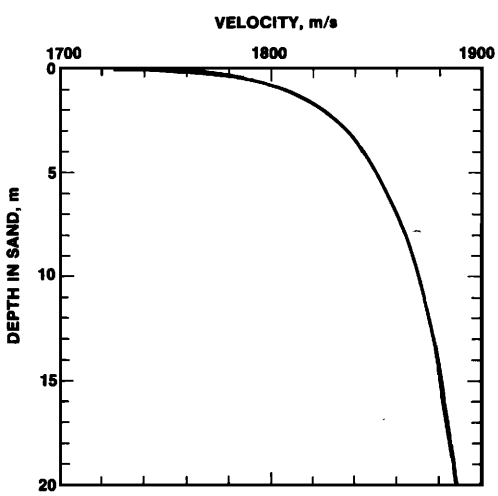

FIG. 7. Compressional wave (sound) velocity versus depth in fine sand. Curve computed from laboratory measurements (see Hamilton[21] for discussion). See Table IV for regression equation.

The presence and values of positive sound velocity gradients in the sea floor are of considerable interest and importance in underwater acoustics and marine geophysics. Where positive velocity gradients are present, and at certain grazing angles, low-frequency sound energy can be refracted through sediment layers and energy returned to the water mass. Some recent studies of sound interactions with the sea floor have emphasized the importance of velocity gradients in reconciling experiments with theory, and in predicting underwater sound propagation.[31-35] Velocity gradients can also be used to compute layer thicknesses and to aid in correlation of sediment and rock layers.

Velocity gradients in a thick sediment layer are usually positive and may be linear, but more often are parabolic, and decrease with depth in the sediments (Ewing and Nafe[36]; Houtz and Ewing[22,37]; Houtz *et al.*[11]; Hamilton[21]; Hamilton *et al.*[13,14]; Houtz *et al.*[12]). It is convenient for purposes of comparison, and to compute thicknesses, to express these gradients as positive, linear increases of velocity with depth, in unit of meters per second per meter, or s^{-1}. The mean velocity gradients, $\overline{a}$, can be computed following the authors cited above, by using instantaneous and mean velocity equations at any given time, t, to compute velocity at various depths, $h\,(h = \overline{V}t)$, in the sediment, and using the relationship (Houtz and Ewing[37]; Houtz *et al.*,[11] Eq. 3)

$$\overline{a} = (V - V_0)/h\,, \tag{1}$$

where V is instantaneous velocity at depth, h.

This equation can be related to the equation for instantaneous velocity vs one way sound travel time (Table III) and the time-integrated instantaneous velocity equation to get h

$$\overline{a} = (V - V_0)/h = (A + Bt + Ct^2 - A)/(At + Bt^2/2 + Ct^3/3)$$
$$= (B + Ct)/(A + Bt/2 + Ct^2/3)\,, \tag{2}$$

Houtz *et al.* (Ref. 11, p. 2637, Eq. 2) noted that

$$a = dV/dh = (B + 2Ct)/(A + Bt + Ct^2)\,, \tag{3}$$

where in Eqs. (2) and (3), A, B, and C are coefficients in the equations for instantaneous velocity versus one-way sound travel time, and A is V_0.

Equation (2) expresses the mean velocity gradient between the sediment surface and any given time, t, whereas Eq. (3) expresses the instantaneous velocity gradient. The two equations are equivalent only at $t = 0$, where the velocity gradient is B/A. The velocity gradients in Table V and in the various figures are mean velocity gradients computed with Eq. (1).

Linear velocity gradients between any two depths can be computed with a velocity–depth equation. This was done for the 20 areas of mostly turbidites. The results are illustrated in Fig. 8. Linear velocity gradients at increments of 0.1 to 0.5 s were also computed and plotted against one-way travel time for the 20 areas of terrigenous sediments, and for siliceous and calcareous sediments (Fig. 9).

The ranges and values of velocity gradients in the 20 areas of terrigenous sediments are about the same as

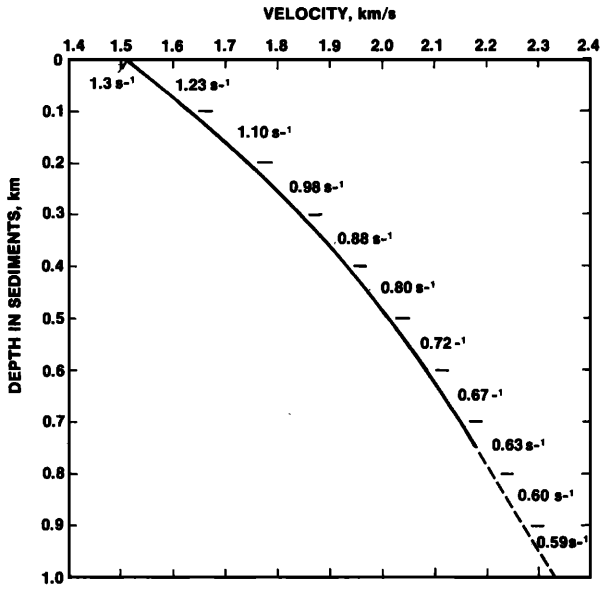

FIG. 8. Sound velocity versus depth in the sea floor in 20 areas of terrigenous sediments and rocks. Linear velocity gradients, in s^{-1}, are shown between 100-m depth intervals.

previously published with fewer areas (Hamilton *et al.*[13,14]). For the 20 areas, the mean values of velocity gradients (Fig. 9) vary from 1.28 s^{-1} at the surface to 0.78 s^{-1} at $t = 0.5$ s. In the data which were averaged, sediment surface values have a total range from 0.7 s^{-1} in the southeastern Bering Sea to 1.99 s^{-1} in the Japan Sea. Within the 95 percent confidence limits, the surface values range from 1.1 to 1.5 s^{-1}, which is very close to those reported by Houtz *et al.*[11]: 1.1 to 1.7 s^{-1} for the Atlantic and adjacent areas.

The averaged velocity gradient in the 20 areas decreases smoothly with depth. In Fig. 8, the average linear gradient is shown between 100 m depth intervals.

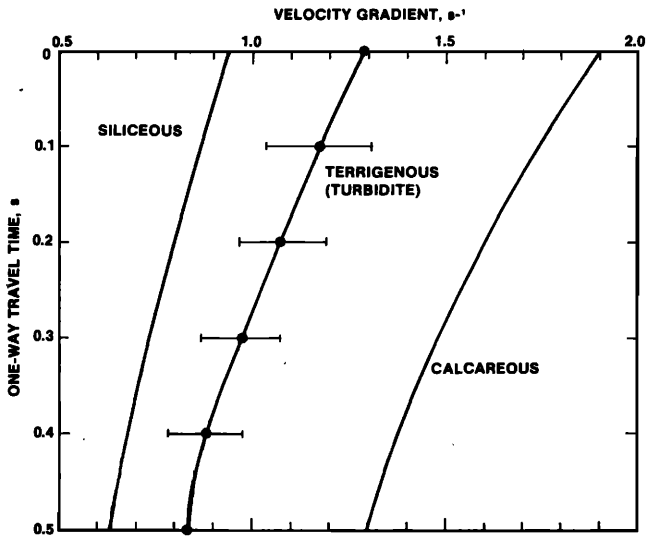

FIG. 9. Linear velocity gradients in meters per second per meter (or s^{-1}) versus one-way sound travel time in the sea floor. These gradients are between the sediment surface and any given travel time. The sediment types are described in Fig. 5. See Table V for regression equations.

These gradients were computed with the velocity versus depth equation in Table IV. As illustrated, these gradients decrease from 1.3 s^{-1} just below the sediment surface to about 0.6 s^{-1} at depths below 700 m. It is probable that at depths below about 300 to 600 m, the sediment is semilithified or lithified, and could be called a mudstone or claystone (reviewed by Hamilton[10]). The velocity gradients in terrigenous materials are intermediate between those for calcareous and siliceous materials (Fig. 9).

The velocity gradients in calcareous sediments and rocks decrease from a value of about 1.9 s^{-1} at the surface to about 1.3 at $t = 0.5$ s. These gradients are appreciably greater than those in siliceous and terrigenous materials (Figs. 5, 9). Houtz *et al.*[12] indicate a surface gradient of about 1.83 s^{-1} in the Equatorial Pacific, where there are thick sections of calcareous sediments.

The smallest velocity gradients and the least changes with depth in the three environments are in the diatomaceous sediments of the Central Bering Sea (Figs. 5, 9). These gradients vary from about 0.9 s^{-1}, at the sediment surface, to about 0.6 s^{-1} at $t = 0.5$ s.

In all sediment types the results of the sonobuoy measurements, as expressed by the regression equations and curves, are averaging the varying velocities in relatively thin layers. This is especially true in turbidites where mud of low velocity usually alternates with thinner layers of higher-velocity silts and sands. This is also true in calcareous materials where relatively soft, low-velocity oozes may be interbedded with chalks, and chalks and oozes interbedded with high-velocity limestones.

Velocity in the sand used as an example in this report increases very fast in the first meter (Fig. 7). Between 1 and 2 m depth the velocity gradient is 19 s^{-1}; between 1 and 20 m the average gradient is about 4 s^{-1}. After the initial rapid increase, the gradient decreases sharply: between 1 and 3 m the gradient is 15 s^{-1}, whereas between 18 and 20 m it is about 1.5 s^{-1}.

The causes of sound velocity gradients in marine sediments were discussed at length by Hamilton.[21] For silt clays and turbidites it was concluded that, to 500-m depth in the sea floor, the pressure-induced porosity reductions and effects on the sediment-mineral frame due to overburden pressure accounted for about 66% of the gradient. The other factors were sound velocity increases due to heat flow and consequent temperature increases with depth (about 17% of the gradient), pore-water pressure increases (about 2%) and increases in rigidity caused by lithification (about 15%).

In thick sections of calcareous materials in the sea floor (sampled by the DSDP), there is usually no smooth transition from soft sediment to chalk to limestone. At rather shallow depths (150 to 300 m), the first chalk may appear, but ooze may be interbedded with chalks, and lower in the hole chalk may alternate with limestone (e.g., Schlanger and Douglas[38]). This causes much scatter around any velocity-depth function in calcareous materials (Johnson *et al.*[39]), and the higher-

velocity chalks and limestones near the sediment surface are a principal reason for the higher velocity gradients in calcareous sections (Figs. 5, 9). After lithification there is apparently little further reduction of porosity with depth (e.g., Hamilton[10]).

In the case of diatomaceous sediments, cementation (without lithification) between siliceous frustules apparently builds up the structural strength of the sediments so that porosity reduction with depth is less than in the other sediments, and as a consequence, velocity gradients are less in these siliceous sediments (the same should be true of radiolarian oozes; Figs. 5, 9).

G. Computations of sediment and rock layer thicknesses

There are two common ways to compute the true thickness of a sediment or rock layer. The first method requires one-way sound travel time through the layer, and the mean velocity in the layer (usually determined from sonobuoy measurements). The second method requires one-way travel time, the velocity of sound in the sediment surface, V_0, and the velocity gradient.

Two-way travel time of sound through a layer ("reflection time") can be measured directly from the acoustic reflection record (e.g., Fig. 10). These times were divided by two to get one-way travel time and listed in the geoacoustic model table under "Thickness, s" in the main table (Appendix A).

The best way to compute thicknesses of the first unlithified sediment layer is to use a sonobuoy measurement of velocity for the specific area, or a number of measurements combined for the specific region. Otherwise one can use regression equations for similar sediment types elsewhere, or use averaged equations for the general sediment type, as discussed in this report (e.g., the 20-area equations), with an appropriate value for V_0. To compute thickness, h, the mean velocity ($\overline{V}$) equations of Table III can be used with one-way sound travel time in the layer, t, as measured from reflection records ($h = \overline{V}t = At + Bt^2 + Ct^3$). The values of thickness shown in the example geoacoustic model table (Appendix A) under "Thickness, m") were computed in this way.

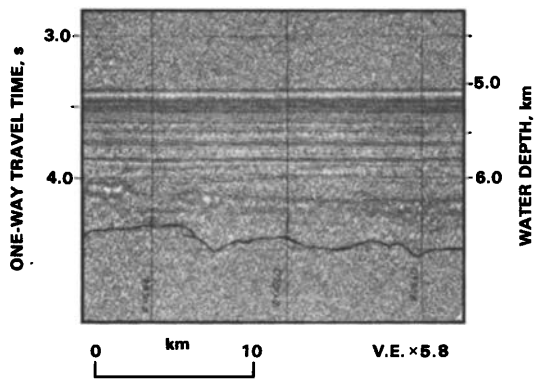

FIG. 10. An example of an acoustic reflection record taken with air-gun sound source in the western Indian Ocean. Sound travel time can be measured directly from such records (see text for discussion).

A second way to compute layer thicknesses is to use the equation (Houtz and Ewing[37]): $h = V_0(e^{\bar{a}t} - 1)/\bar{a}$. The sediment surface velocity, V_0, can be determined from core measurements or tables and corrected to *in situ* values (as discussed above); one-way sound travel time can be measured from reflection records, and a predicted value for the velocity gradient, $\bar{a}$, can be derived from Table V or Fig. 9.

H. Surface sound channels in marine sediments

When the sediment surface velocity, V_0, is less than that in the bottom water, V_w, and there is a positive velocity gradient, $\bar{a}$, a small sound channel can be formed in the top of the first sediment layer (Hamilton[40]). The height of this sound channel, h_{sc}, depends on the velocity ratio, R, and on the velocity gradient: $h_{sc} = (V_w - V_0)/\bar{a} = V_w(1 - R)/\bar{a}$. For the 20 areas of terrigeneous sediments (R about 0.99, V_0 about 1511 m/s, V_w about 1526 m/s, and $\bar{a}$ about 1.3 s^{-1}) there should be a sound channel averaging about 12 m high. In pelagic clay, assuming a bottom-water velocity at about 5000 m water depth (1542 m/s), and a velocity ratio of 0.984 (Hamilton,[10] p. 298, average of all samples), and using various velocity gradients from 1.0 to 1.3 s^{-1}, the height of the sound channel should be 19 to 25 m; if the velocity gradient is as low as 0.5 s^{-1}, the sound channel could be as high as 50 m. Sediment surface velocities in diatomaceous sediments (Bering Sea) and calcareous sediments (Equatorial Pacific) are so close to (or greater than) bottom-water velocities that no sediment sound channel can be predicted.

I. Shear wave velocity

Shear wave velocity, or dynamic rigidity, of sediments was not a required property in many older bottom-loss models (and some simpler models still in use). However, in recent years, it has been shown that shear wave velocities and rigidity are important properties for more sophisticated mathematical models involving sound interactions with the sea floor (Bucker and Morris[41]; Hawker and Foreman[42]; Hawker *et al.*[35,43]; Hawker[44,45]; Vidmar and Foreman[46]).

In previous papers (Hamilton[29,30]), the presence and causes of dynamic rigidity (shear modulus) and shear waves in marine sediments was reviewed. It was concluded that almost all marine sediments possess enough rigidity to transmit shear waves, and that there was negligible velocity dispersion in compressional waves (the same should be true of shear waves). Shear waves are important in underwater sound propagation because compressional waves can be partially converted to shear waves or Stoneley waves at reflection boundaries, and the energy is rapidly attenuated (see references above). In the present discussion, only low-strain shear waves (less than about 10^{-5} or 10^{-6}) are considered. These are the strains expectable when sound waves pass through earth materials.

The velocity of shear waves in the first layer of sediments and in lower layers of sedimentary rocks can be approximately predicted by the relations between compressional and shear waves from a recent study (Hamil-

ton[47]). The basic information on shear wave velocity versus depth (to 650 m) in silt-clays and turbidites (Fig. 11), came from a review (Hamilton[30]); three linear equations were used to characterize the data. Also shown in Fig. 11, for comparison, is a curve for shear wave velocity versus depth in clays and silty soil from Ohta and Goto.[48] The data came from a large number of *in situ* measurements in the alluvial plains of Japan. The regression equation for the Japanese data is: $V_s = 78.98D^{0.312}$; where V_s is in m/s, and D is depth in m.

The shear wave velocities (Hamilton[30]) were linked at common depths to the compressional wave-velocity-versus-depth data for 20 areas of silt-clays and turbidites which were discussed above and illustrated in Fig. 4. Regression equations could then be derived which linked compressional and shear wave velocities to depths of about 600–700 m. The resulting curves of compressional velocity versus shear velocity are shown in Fig. 12. The linear curve between compressional velocities of about 2.15 and 3.4 km/s was extrapolated on very little data.

The regression equation of compressional wave velocity, V_p, and shear wave velocity, V_s, in km/s, for silt-clay sediments and sedimentary rocks such as mudstone and shale are,

from $V_p = 1.512$ to 1.555 km/s:

$$V_s = 3.884V_p - 5.757, \quad (4)$$

from $V_p = 1.555$ to 1.650 km/s:

$$V_s = 1.137V_p - 1.485, \quad (5)$$

from $V_p = 1.650$ to 2.150 km/s:

$$V_s = 0.991 - 1.136V_p + 0.47V_p^2, \quad (6)$$

V_p greater than 2.150 km/s (dashed line in Fig. 12):

$$V_s = 0.78V_p - 0.962. \quad (7)$$

The use of *in situ* V_p and V_s data versus depth in the sea floor has the advantage of "built-in" temperature and pressure corrections, and in allowing for the effects of reduction of sediment porosity with increasing overburden pressures. When the sediment surface compressional velocity is less than 1.51 km/s, the shear wave velocity can be approximated with a V_p/V_s ratio of 13 (the ratio at the water–sediment interface predicted by the data in Hamilton.[47]) At compressional wave velocities greater than 3.4 km/s, a V_p/V_s ratio of 2.0 can be used.

The data illustrated in Fig. 12 and defined in Eqs. (4)–(7) apply to terrigenous materials. In the absence of sufficient data, the same equations are recommended for use in predicting shear wave velocities in calcareous ooze and pelagic clay.

When the rock type is considered to be chalk or limestone, a V_p/V_s ratio of 1.90 (Hamilton[47]) can be used with the compressional wave velocity to predict shear wave velocity.

In a detailed model of a thin layer of silt clay (less than a meter to about 40 m), the value of V_s at the bottom of the layer can also be established by using a variation of an equation in Hamilton[30] (Eq. 2, p. 990): $V_s = V_{s,\,\mathrm{sfc}} + 4.65D$; where V_s is in m/s, and depth, D, is in m.

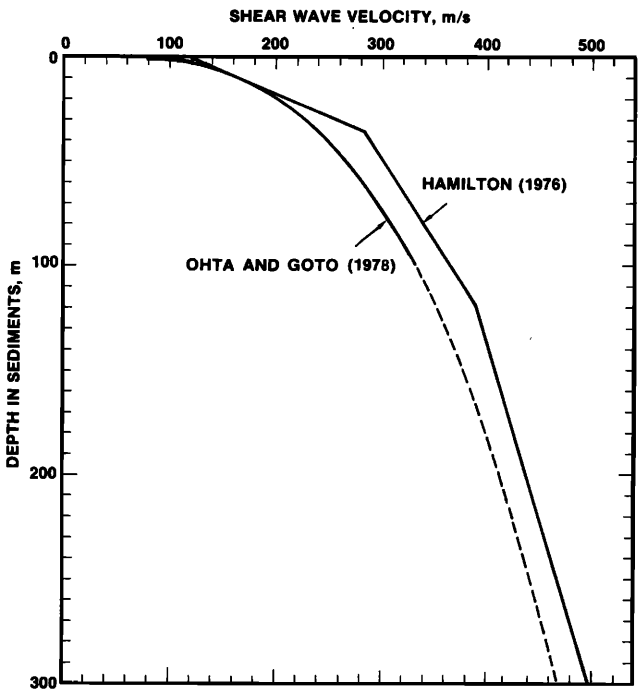

FIG. 11. Shear wave velocity versus depth in selected water-saturated silt-clays and turbidites. The solid lines represent three regression equations. One measurement ($V_s = 700$ m/s at 650 m) is not shown. See Hamilton[30] for regression equations and discussion. The curve from Japan is shown for comparison (see text for regression equation).

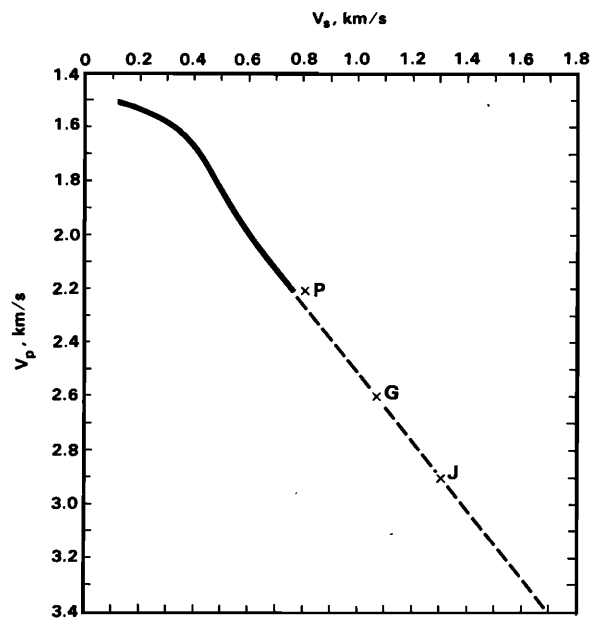

FIG. 12. Compressional wave velocity, V_p, versus shear wave velocity, V_s, in terrigenous marine sediments (mostly silt-clays, turbidites, mudstone-shale). The solid curve represents three regression equations (see text). The dashed line is extrapolated on very little data; the letters "P", "G", and "J", represent Pierre shale (McDonal *et al.*[59]), Grayson shale (Geyer and Martner[94]), and data from a deep borehole in Japan (Yamamizu *et al.*[95]).

The equations of Christensen and Salisbury[49] from measurements in basalts drilled by the Deep Sea Drilling Project can be used to predict shear wave velocities in basalts, given values of compressional velocity from the literature. The findings of Christensen and Salisbury (at a pressure of 0.5 kbar) are illustrated in Fig. 13. An equation computed from these data is illustrated in Fig. 14; the equation (velocities in km/s) is

$$V_s = 0.531 + 0.2077 V_p + 0.374 V_p^2. \quad (8)$$

It should be emphasized that the laboratory measurements of Christensen and Salisbury[49] in basalts were in hand samples, whereas the field measurements by seismic methods are in large volumes of rock. Hyndman and Drury[50] and Francis[51] have reported measurements of V_p and V_s in the Mid-Atlantic Ridge crestal area. They emphasize that low V_p values in such areas may reflect the presence of large-scale fissures and cracks, as well as volcanic detrital material mixed with normal sediments. Away from such ridges (where new sea floor is being added), the cracks and fissures are thought to be filled with sedimentary material, and the consequent compressional velocities higher (e.g., Talwani *et al.*[52]; Houtz[53]). In a report on velocity–density relations in the sea floor (Hamilton[54]), these subjects are discussed in detail. The data of Christensen and Salisbury[49] should be more representative of *in situ* conditions in the top of the basaltic crust away from ridges.

When the sediment body being modeled is considered

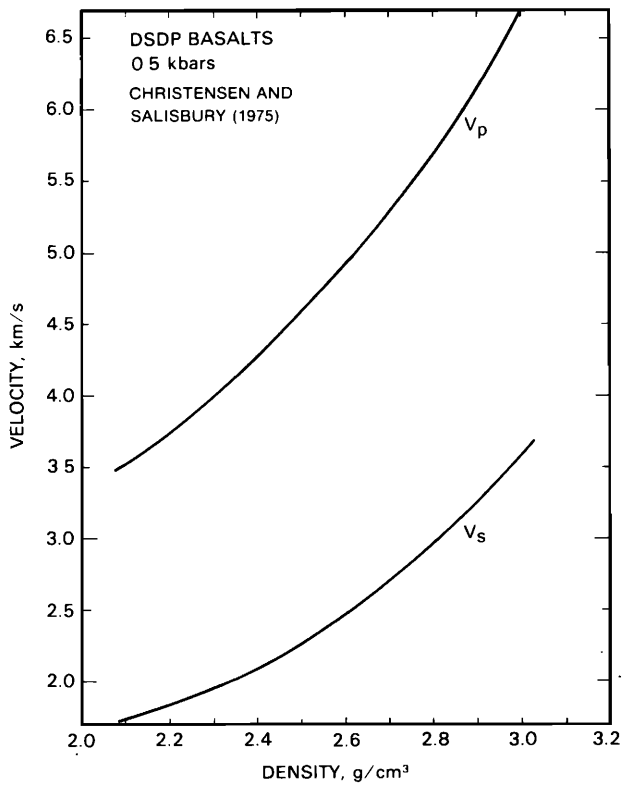

FIG. 13. Compressional wave velocity and shear-wave velocity versus density in basalts from the boreholes of the Deep Sea Drilling Project at an effective pressure of 0.5 kbar (from Christensen and Salisbury[49]). See Christensen and Salisbury or Hamilton[54] for regression equations.

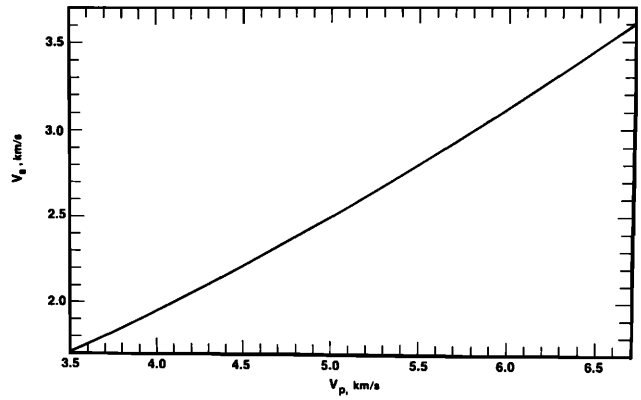

FIG. 14. Compressional wave velocity, V_p, versus shear wave velocity, V_s, in laboratory samples of water-saturated basalts from the Deep Sea Drilling Project at a pressure of 0.5 kbar (from Christensen and Salisbury[49]). See text for regression equation.

to be sand, shear wave velocities can be approximated by the relations between compressional and shear wave velocities from a recent study (Hamilton[47]). Compressional wave velocities in fine sand as a function of depth in the sand body were previously discussed and illustrated (Fig. 7). In a previous report (Hamilton[30]), *in situ* shear wave velocity versus depth in mostly fine sands was generalized in the regression equation: $V_s = 128 D^{0.28}$; where D is depth in m, and V_s is in m/s (Fig. 15). Also shown in Fig. 15, for comparison, is a curve for shear wave velocity as a function of depth in fine, medium, and coarse sands in Japan (Ohta and Goto[48]). The regression equation (averaging the three kinds of sands) is: $V_s = 104.33 D^{0.312}$. Figure 16 illustrates V_p vs V_s when the data in Figs. 7 and 15 are linked at common depths in sands.

J. Attenuation of compressional waves

1. *Introduction*

When sound is refracted through the sea floor due to positive velocity gradients and/or higher-velocity layers

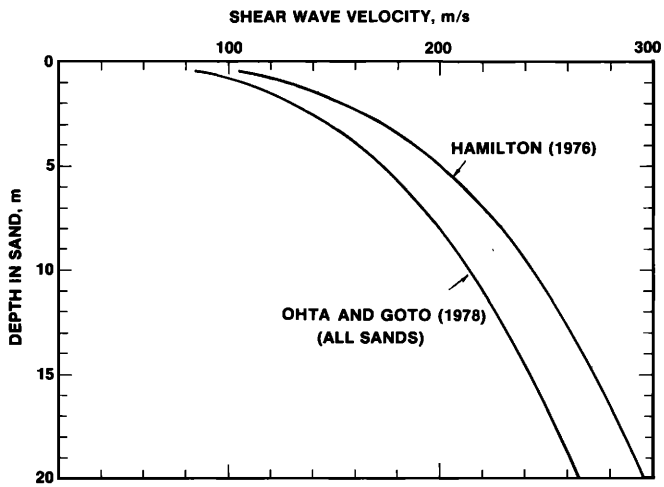

FIG. 15. Shear-wave velocity versus depth in selected water-saturated sands. The curve from Japanese data is shown for comparison. See text for regression equations. See Hamilton[30,47] for discussion.

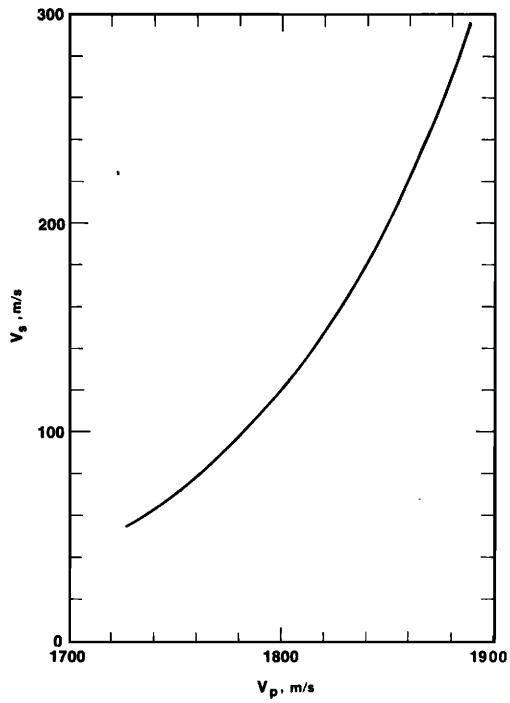

FIG. 16. Compressional wave velocity, V_p, and shear wave velocity, V_s, in selected water-saturated sands. The regression equation is: $V_s = 21.05 - 24.617V_p + 7.215V_p^2$; where V_p and V_s are in km/s; see Hamilton[47] for discussion.

at depth, or is reflected from impedance mismatches within the sediment or rock body, energy is returned to the water mass. The amount of returned energy depends on the sound path length and attenuation of sound along the path. Consequently, sound attenuation at the sediment surface, and as a function of depth in the sea floor, are important components of geoacoustic models.

2. *Attenuation versus frequency*

Figure 17 illustrates a large collection of data on attenuation versus frequency in unlithified marine sediments. This figure is revised from previous publications (Hamilton[2, 55, 56]). The newly added data are indicated with open symbols or dashed lines to indicate the impact of the data added since 1972. The latest data are those of Bjorno[57] who measured attenuation in medium, fine, and very fine sands, and in silt at 10 and 100 kHz. He found an approximate linear relationship between attenuation and frequency.

The line labeled "f^1" in Fig. 17 indicates the slope of any line representing a first power dependence of attenuation on frequency. It can be seen that most of the data are consistent with an approximate first-power dependence of attenuation on frequency over a frequency range from below 10 Hz to 1 MHz. The upper and lower bounds of the data plot probably define the area

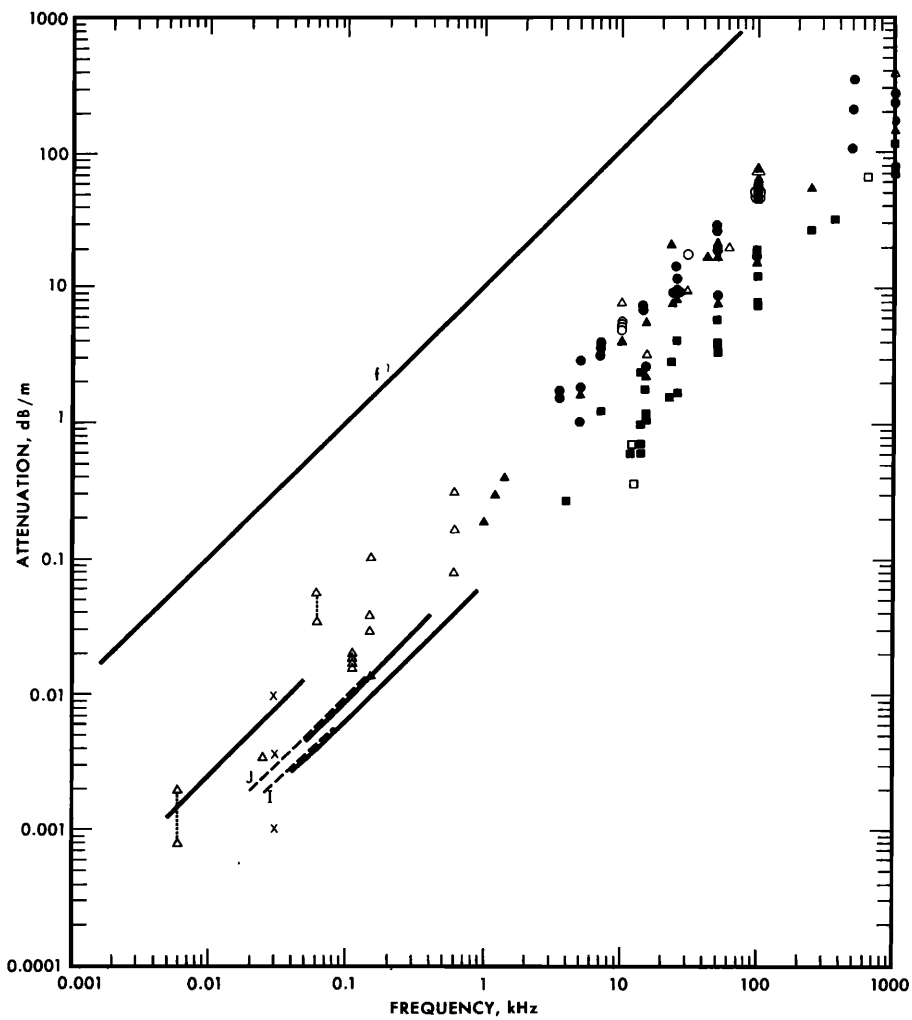

FIG. 17. Attenuation of compressional waves versus frequency in natural, saturated sediments and sedimentary strata. Symbols: circles—sand (all sizes); squares—clay-silt (mud); triangles—mixed sizes (e.g., silty sand, sandy silt). Open symbols have been added since original publication of the figure (Hamilton[55]); the latest data are for four sands and a silt from Bjorno[57] at 10 and 100 kHz. The line labeled "f^1" indicates the slope of any line having a dependence of attenuation on the first power of frequency. For other symbols and discussions see Hamilton[2, 55, 56] and this text.

in which most natural marine sediments will lie. With regard to sediment type, the silt-clays or "mud" (squares) lies in a narrow band along the lower side of the plot, and the sands (circles), and mixtures such as silty sand, sandy silt, etc., (triangles) lie along the top. These different sediment types are shown on the same plot for convenience. Not shown on the plot are data from lithified sediments such as mudstone and shale which also indicate an approximate first-power dependence of attenuation on frequency (Kudo and Shima[58]; McDonal *et al.*[59]).

In studies and discussions of the dependence of sound attenuation on frequency it is necessary to distinguish between sediment types. In silt-clays (mud) and their lithified equivalents (mudstone, claystone, shale) both theory and experimental evidence indicate an approximate first-order dependence of attenuation on frequency from very low to high frequencies; a few Hz to the MHz range (Hamilton[2,55,56]; Stoll and Bryan[60]; Stoll[61,62,63]).

Stoll[63] found the logarithmic decrement of shear waves in a water-saturated silt to be independent of frequency for low-amplitude waves at frequencies between 43 and 391 Hz; this also indicates a first-order dependence of attenuation on frequency for both shear and compressional waves. In similar sediments (silt) at about the same porosity, Bjorno,[57] at frequencies of 10 and 100 kHz, found a first-order dependence of compressional waves on frequency. These later data are in accord with the silt data shown in Fig. 17. Since silt–clays form the major portion of deep sea abyssal plains, with relatively thin layers of silt (the most common layer), it appears that both theory and experiment call for an approximate first-order dependence of attenuation on frequency in most turbidites. This is affirmed by *in situ* measurements. The excellent measurement of Tullos and Reid,[64] for example, were in this type of material (clay–sand) and called for a first-power dependence in the frequency range of 50–400 Hz. Neprochnov[65] in his summary of a great deal of Soviet data on attenuation in thick turbidite layers in the sea floor, remarked that as a rule, a linear relationship was found between attenuation and frequency in the frequency range from 20–400 Hz.

It appears that the only area of disagreement among investigators of attenuation in water-saturated sediments is for sands. In a study of attenuation in marine sediments, including sands, Hamilton[1,2,55,56] considered that the best evidence indicated that attenuation was approximately related to the first power of frequency. This appears to be true for natural, water-saturated sands in the frequency range from about 1–100 kHz, and probably to the MHz range (e.g., Hamilton[1,2,55,56]; McLeroy and DeLoach[66]; McCann and McCann[67]). The latest data for sands in this frequency range (10 and 100 kHz) are those of Bjorno[57] who found a linear relationship. However, Stoll and Bryan,[60] and Stoll[61,62,63] following Biot[68,69] favor a theoretical model for sands calling for an f^2 dependence at low frequencies and $f^{1/2}$ at high frequencies with the inflection in the curve somewhere between 1 and 10–20 kHz. The number of studies of attenuation in sands from 1–100 kHz affirm an approximate first-power relationship between attenuation and frequency, and deny any $f^{1/2}$ relationship as called for by Stoll[62] in this frequency range. There are no measurements of attenuation of compressional waves in the low-frequency range (1–1000 Hz) in water-saturated, poorly-sorted, natural sands which confirm or deny Stoll's conclusions that there is an f^2 dependence in this range of frequencies in sands. In this low range the evidence is conflicting for measurements of attenuation of shear waves. Stoll[63] in an excellent study of shear wave energy losses indicates that in clean, highly permeable sands at frequencies of 30–340 Hz, viscous losses due to relative movement of pore water and mineral may cause attenuation to be nearer f^2 at low frequencies. However, Kudo and Shima[58] measured the attenuation of shear waves in diluvial natural sands *in situ* at frequencies between 30 and 80 Hz and found no velocity dispersion and Q independent of frequency (attenuation proportional to the first power of frequency).

In summary (regarding the dependence of attenuation of compressional waves on frequency in marine sediments), Stoll (Refs. 62 and 63), and Hamilton (Refs. 1, 2, 55, 56 and in this report) agree that there is an approximate first-power dependence of attenuation on frequency in silt clays (mud) from low to high frequencies. Turbidites (lumped with sands by Stoll[62]) are mostly silt–clays and silts (except in and near Abyssal-Plain channels and in coastal areas) and fall in the category (with silt-clays) of first-order dependence. Inasmuch as the experimental evidence of attenuation and frequency from 1–100 kHz (and probably to 1 MHz) in sands indicates an approximate first-power dependence, the only valid area of disagreement remaining is for natural, *in situ* sands in the low-frequency range. Hovem,[70] Hovem and Ingram,[71] and Bell,[72] may have the answer to this problem when they noted that energy losses due to relative movement of pore water and sediment mineral frame (leading to an f^2 dependence of attenuation at low frequencies) may be of potential importance only in sound propagation in sands with rather uniform grains and high permeability. Fortunately, for modeling purposes, sands cover a relatively small part of the sea floor: mostly in shallow water, and in or near abyssal plain channels. Most of these sands are poorly sorted, and have lower permeabilities than do clean, uniform-sized laboratory sands. However, this matter should be cleared up with carefully controlled, *in situ*, experiments of sound attenuation in natural seafloor sands at frequencies from a few Hz to 1 kHz.

3. Attenuation versus sediment porosity and grain sizes

The predicted values of attenuation of compressional waves for the sediment surface in models are usually based on published relationships between attenuation and sediment porosity or mean grain sized (Hamilton[1,2,55,56]). In these reports attenuation of compressional waves, α_p, in dB/m, was related to frequency, f, in kHz, through a constant k_p, in the equation

$$\alpha_p = k_p f. \tag{9}$$

The case was made in these reports that attenuation was approximately related to the first power of frequency. In which case the only variable in Eq. (9) is the constant k_p (in units of dB/m/kHz). This constant varies with the sediment type and is related to porosity and mean grain diameter (Figs. 18 and 19 are reproduced from the 1972 and 1976 reports with data from Bjorno[57] added). The values of porosity, n, as a decimal fraction, (from coring data), can be used to enter the equations for k_p versus n, in the equations in Hamilton[55] (Fig. 5 caption).

The values from the equations of k_p vs porosity are listed in the main geoacoustic model table (e.g., Appendix A) as surface ("*Sfc*") values. These values are recommended for first-trial use by acousticians in reconciling experiments with theory. However, as noted in the 1972 report[55] (p. 635, and caption to Fig. 3), there is much scatter in the data and, therefore, predictions have to include a probable range based on the dashed lines above and below the regression curves (Figs. 18, 19). Consequently, in the main table for each model (e.g., Appendix A) there are usually three values listed under "k_p." The center value is recommeded for first-trial use by acousticians, the left-hand value is probable minimum, the right-hand value is probable maximum. There is some indication that in the higher porosity silt-clays and turbidites that the usual range of k_p values should be in the low part of the range; namely from the bottom dashed line to the center (regression) line. This subject is discussed in the next section.

At the present time, in view of the scatter in the data, and small amount of *in situ* measurements of effective attenuation, the acoustician is justified in selecting attenuation constants for the surface within the stated range in comparing his field experiments with theory However, it appears at this time that most future surficial data for high-porosity, deep-sea sediments will fall into the lower part of the range, between 0.03 and 0.10.

It has been noted that the equations relating mean grain size and k_p (Fig. 19, Hamilton,[55] Fig. 3 and its caption) will frequently yield lower values of k_p than will porosity for the same sediment. Thus, the expectable lower limit of k_p in higher-porosity sediments in the mean-grain-size versus k_p diagram (Fig. 19) is about 0.03.

Recently, measurements of effective compressional wave attenuation in sediment wedges at 4 kHz have been made by Tyce[73] in various sea-floor environments using the Marine Physical Laboratory (University of California) Deeptow instrument package (see Tyce's detailed results in this series of papers). Porosities and mean grain sizes in sediments cored in some of these areas, when entered in the k_p versus porosity and mean-grain-size diagrams, yielded reasonably close predictions of

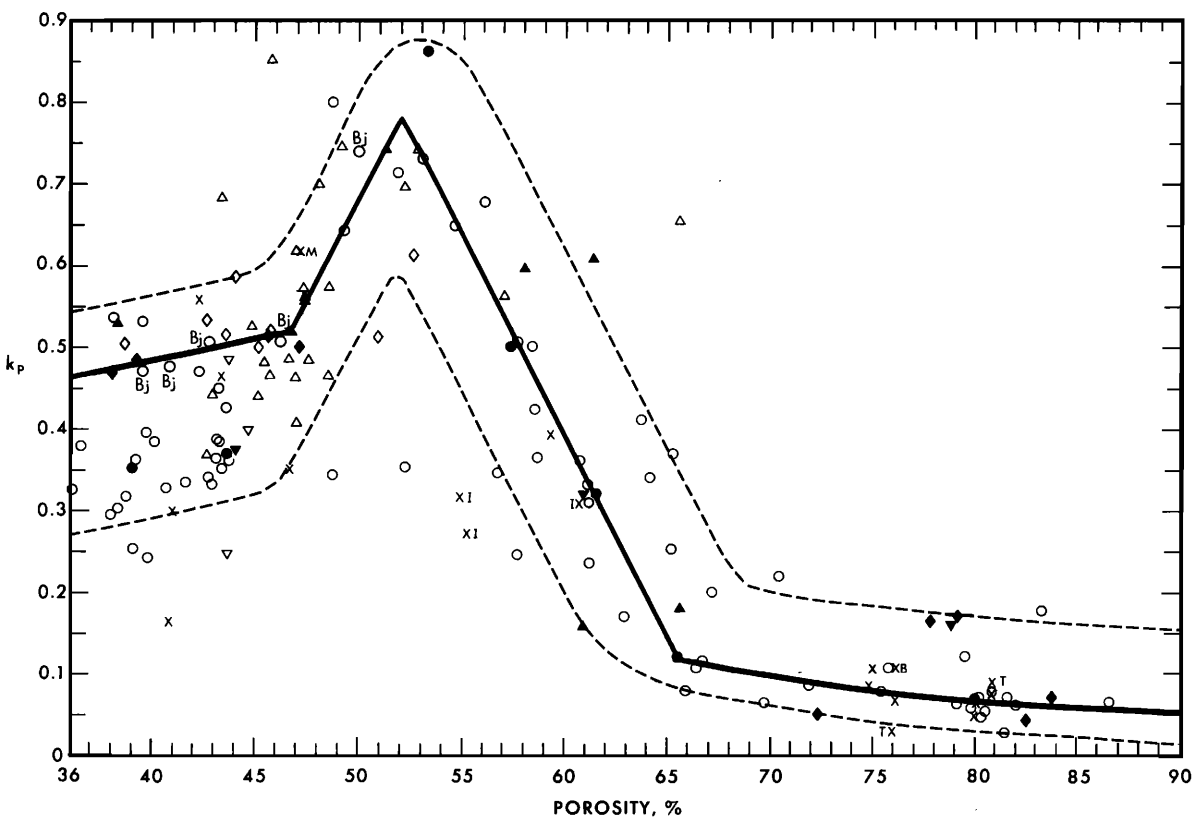

FIG. 18. Attenuation of compressional waves (expressed as k_p in α_p, in dB/m=$k_p f$, where frequency, f, is in kHz) versus porosity in natural, saturated surface sediments. Solid symbols are averages and open symbols are the averaged data from measurements off San Diego; solid lines are regressions on the best data (from Hamilton[55], Fig. 5); *X* indicates values from the literature. The dashed lines represent areas into which it is predicted most data will fall. Regression equations are included in the caption to the original figure.[55] Newly added data are indicated by letters next to symbols (see Hamilton[56] for references); the latest data (from Bjorno[57]) in four sands and one silt are indicated by open circles with a "B_j," between porosities of 39% and 50%.

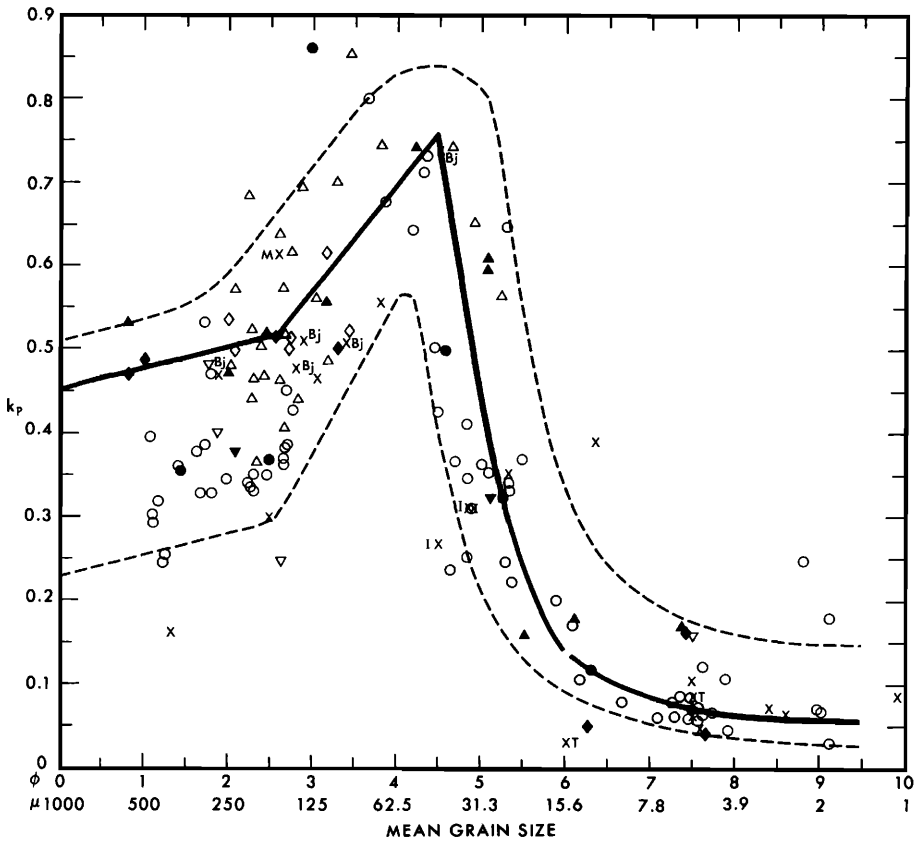

FIG. 19. Surface-sediment mean grain size versus attenuation of compressional waves (expressed as k_p, defined in Fig. 18). The symbols and lines are as indicated in Fig. 18. For additional information and regression equations see Hamilton.[55]

the actual attenuation measurements, although Tyce's measurements must be considered as effective attenuation rather than intrinsic attenuation (as discussed in the next section). An overall conclusion from Tyce's data is that his measurements favored the lower part of the range of values of k_p (0.05 to 0.20) which might have been predicted from Hamilton[55]; namely, his overall range was 0.03–0.16. Without one value of 0.16, the range was 0.03 to 0.10.

4. Attenuation versus depth in the sea floor

a. Attenuation versus depth in the sea floor. When low-frequency sound is transmitted through sediment and sedimentary rock layers of the sea floor, sound energy is lost through a number of mechanisms. The more important of these have been excellently summarized by Sheriff.[74] Some of these are (in addition to spreading losses):

(i) *Intrinsic absorption or attenuation*—the intrinsic attenuation as sound energy passes through materials due to conversion of energy into heat, which is quickly dissipated. This is the cause of energy losses discussed by Hamilton.[55]

(ii) *Transmission through reflectors* (including multiple reflections, "peg-leg multiples")—these reflection and refraction losses (and reinforcements) also include conversion of compressional to shear waves and consequent rapid attenuation.

(iii) *Reflector roughness and curvature*—focusing and defocusing effects of concave and convex reflectors (easily seen on any echo sounder or acoustic reflection record).

(iv) *Scattering by inhomogeneities* within the sediment or rock body, or along reflector surfaces.

In other words, when low-frequency sound of sufficient energy goes into the sea floor, it loses energy through many causes, only one of which is intrinsic attenuation in the various materials. The total of all the losses (excluding spreading losses) is called "effective attenuation."

Very little data are available to determine compressional wave effective attenuation as a function of depth in the sea floor. That available was collected and interpreted (Hamilton[56]). Figure 20 is reproduced from that report. It appears from this study and later work by Tyce[73] that there is little difference in sediment surface values of intrinsic attenuation and effective attenuation in the first few tens of meters in the sea floor.

As briefly discussed in the preceding section, the relations between the constant k_p in Eq. (9) and sediment physical properties have furnished a useful means of extrapolating measurements and predicting attenuation. The constant k_p will be used in this section to discuss the variations of attenuation with depth in the sea floor.

Figure 20 illustrates the available published data (listed and referenced in Hamilton[2,55,56]) on the variations of attenuation (expressed as k_p) at the surface and at depth in silt clays, turbidites, sedimentary rocks,

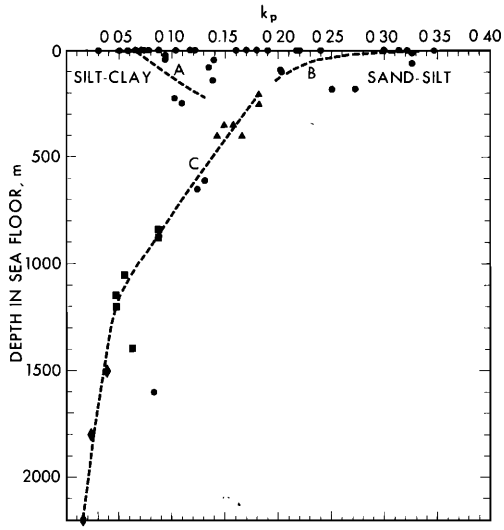

FIG. 20. Attenuation of compressional waves (expressed as k_p, defined in Fig. 18) versus depth in the sea floor, or in sedimentary strata. For discussion of symbols and curves see Hamilton.[56] Symbols: circles—measurements from the literature; triangles—squares, and diamonds represent the first, second, and third layers, respectively, in the sea floor in seven areas (from Neprochnov[65]).

and basalts in the sea floor. Not shown on Fig. 20 are all the values of k_p for sands and mixed sands and silts; values of k_p in these materials usually range from about 0.3 to about 0.9 (see Fig. 18). Sand bodies in the sea floor are usually relatively thin compared to thick silt-clay and turbidite sections, and the gradients of attenuation in sands are better known than in silt-clays. All data were converted, if necessary, into the form of Eq. (9), and then k_p was computed. Where attenuation was given for an interval or layer, the value was plotted at $\frac{1}{2}$ the interval thickness for the first layer, or to the midpoint of a lower layer. As a result, the data in Fig. 20 form curves of instantaneous attenuation as a function of depth in the sea floor.

Noprochnov (Ref. 65, p. 711) presented attenuation data for thick sediment and rock layers, in the frequency range of 20 to 200 Hz, for 7 areas in the Indian Ocean, Black Sea, and Japan Sea. In Fig. 20, the Soviet data are given special symbols. The first layers, which should all be unlithified sediments, are indicated by triangles; the second layers, dominantly sedimentary rock (probably mudstone), are indicated by squares; and the third layers, indicated by diamonds, are sedimentary rock and basalt. These layer identifications are based on Deep Sea Drilling Project Sites in the various areas.

Two values of k_p between 600 and 700 m are from measurements on land. A value of k_p (0.13) for the Pierre shale (McDonal *et al.*[59]) is plotted at 610 m (0 to 1219 m), and a value of 0.12 at 650 m (400–900 m) for "clays, sandstone, and aleurolites (mudstone)" from Zhadin (in Vassil'ev and Gurevich[75]).

In silt-clays there is probably a distinctly different variation of attenuation with depth or overburden pressure in the sea floor. The data indicate a probability that attenuation *increases* with depth from the sediment surface to some depth where the pressure effect becomes dominant over reduction in porosity. This subject is discussed in detail in the 1976 report.[56]

Values and gradients of attenuation in silt–clay layers in the sea floor can be approximated as follows. Select a value of k_p at the sediment surface based on porosity or grain size. Attenuation should increase from this value to about 100–400-m depth (roughly parallel to curve A in Fig. 20) and thereafter decrease gradually with depth as with curve C. For sedimentary rocks below about 400 m, use curve C to establish values of k_p. If desirable, minimum, recommended, and maximum values of k_p at the surface can be used as initial points from which lines can be drawn, as above, to an intersection with curve C.

As previously noted, all but two measurements of attenuation below about 200 m are from older Soviet data. It is important that additional measurements of attenuation as a function of depth be made, and some unpublished data are currently being analyzed. Results from the Applied Research Laboratories in Austin are on the very low side of the data in Fig. 20. Jacobson, at the NORDA Symposium, showed data from the Bengal Fan which lie closer to the data in Fig. 20.

Hamilton[55,56] indicates that in surface sands, k_p varies between about 0.25 and 0.60, with a regression on the best data around 0.5. As discussed in Hamilton,[56] and following Gardner *et al.*,[76] it appears that attenuation in sands decreases with about the $-\frac{1}{6}$ power of overburden pressure. Curve B shown in part in Fig. 20 was computed for a fine sand using an average value of k_p (0.45), off the figure to the right, for four stations in fine sands off San Diego at 1-m depth, and assuming a decrease in k_p with the $-\frac{1}{6}$ power of depth. To predict values of attenuation in sand, select a value of k_p at the surface (Figs. 18,19), and then decrease this value with the $-\frac{1}{6}$ power of depth in the sand body.

5. *Attenuation in chalk, limestone, and basalt*

Data on attenuation of compressional waves in limestone are rare. Data from Peselnick and Zeitz[77] for Solenhofen limestone (a very low porosity, dense limestone) indicate that k_p is 0.02 to 0.05 (the same as in basalt). For hard, dense limestone, a value of 0.02 should probably be favored. Evison (in Vassil'ev and Gurevich[75]) measured *in situ* attenuation in chalk which yields a k_p value of 0.08.

Attenuation of compressional waves in basalt is important in geoacoustic modeling because this rock type forms the acoustic basement in most of the world's ocean. Values of k_p in basalts from various laboratory studies (e.g., Balakrishna and Ramana[78]; Levykin[79]) and measurements in the field (e.g., Neprochnov *et al.*[80]; Neprochnov[65]) where the nature of the material is identified by the Deep Sea Drilling Project, geographic location, stratigraphic position, and velocity, indicate that k_p in basalts under the sea floor should usually vary between 0.02 to 0.05. In modeling basalt, a value of 0.03 is recommended for k_p, except when the sedi-

mentary rock above the basalt is 0.02; in this case a value of 0.02 is recommended for the basalt.

K. Attenuation of shear waves

When a compressional wave is reflected at some impedance mismatch within the sea floor, some of the energy is converted to a shear wave and this converted energy is rapidly attenuated.

In some sophisticated mathematical models of sound interaction with the sea floor, the attenuation of shear waves is a required input. The few data available on this subject were summarized and reviewed by Hamilton.[81] In this study the logarithmic decrement was used as a measure of energy losses because of the research which has been done on it in the field of soil mechanics and foundation engineering. The data allowed only generalized averaged values in sands, silt clays, mudstone, and shale.

One of the best *in situ* studies of shear waves in natural, saturated sediments was that of Kudo and Shima[58] in Tokyo. They found in sands, silt, and mudstone, that attenuation of shear waves was near a dependence of f^1 at frequencies of 15–90 Hz. In diluvial sand (glacial-age, water-deposited sands) they found (at 30–80 Hz) negligible or no velocity dispersion and Q independent of frequency (attenuation proportional to f^1). Bell[72] in laboratory studies of shear wave velocity and attenuation in water-saturated glass beads and natural sands, in the frequency range of 1–10 kHz, found shear wave attenuation approximately dependent on the first power of frequency, and no velocity dispersion. McDonal *et al.*,[59] found a first-order dependence of shear wave attenuation on frequency in the frequency range of 20–125 Hz in Pierre shale.

On the other hand, Stoll[63] measured the logarithmic decrement of shear waves in sands and silt in the laboratory at low frequencies (43–391 Hz) and found that, although the log decrement was independent of frequency in silt, measurements in saturated sands of higher permeability at 30–340 Hz indicated viscous losses which caused the log decrement to be dependent on frequency (attenuation not dependent on the first power of frequency).

In other words, Stoll,[63] at low frequencies, found the log decrement of shear waves in sands varied with frequency, but Kudo and Shima,[58] at similar frequencies, found the log decrement to be independent of frequency (or attenuation dependent on the first power of frequency). As in the case of attenuation of compressional waves, additional low-frequency to high-frequency measurements are needed to resolve the dependence of shear-wave attenuation on frequency; especially for mixed sizes of natural *in situ* sands. It may be that the answer lies mostly in permeability of the sands in question (as noted by Stoll[63]; Hovem[70]; Hovem and Ingram[71]; and Bell[72]) and that the highly mixed sizes of natural sands of lower permeability than clean, well-sorted sands of the laboratory have attenuations of shear waves nearer f^1 than f^2 at low frequencies, or $f^{1/2}$ at high frequencies (as found by Kudo and Shima at low frequencies, and by Bell at high frequencies).

For computations and predictions of shear wave energy losses in natural, poorly sorted sands, in silt-clays, mudstone, and shale, it is recommended (pending further measurements) that attenuation of shear waves be considered to vary as the first power of frequency.

In the 1976 report,[81] it was concluded from the sparse data that the logarithmic decrement of low-strain shear waves in most near-surface, natural sands should vary between 0.1 and 0.6, with the most values between 0.2 and 0.4. If approximate values of shear-wave energy losses in sands are required in generalized computations, a value of the log decrement, $\Delta_s = 0.30 \pm 0.15$, can be assumed and used with shear wave lengths to derive values of attenuation (e.g., with Eqs. B4 and B8 in Appendix B). In silt-clays the few data indicate that the logarithmic decrement of low-strain shear waves lies between 0.1 and 0.6 (as in sands); probably most values lie between 0.1 and 0.3. For computations and predictions of shear wave energy losses in silt-clays, a value of the logarithmic decrement, $\Delta_s = 0.2 \pm 0.1$ is recommended.

Assuming that linear attenuation of low-strain shear waves is approximately proportional to the first power of frequency, some of the shear wave enery-loss data from the literature can be placed in the form: $\alpha_s = k_s f$, where the attenuation of shear waves, α_s, is in dB/m; frequency, f, is in kHz, and k_s is a constant. Examples computed by the writer are:

Material	k_s in $\alpha_s = k_s f$	Reference
Diluvial sand	13.2	Kudo and Shima[58]
Diluvial sand and clay	4.8	Meissner[82]
Alluvial silt	13.4	Kudo and Shima[58]
Mud (silt-clay)	17.3	Warrick[83]
Water-saturated clay	15.2	Molotova[84]
Tertiary mudstone	10.1	Kudo and Shima[58]
Pierre shale	3.4	McDonal *et al.*[59]
Solenhofen limestone	0.02 to 0.05	Peselnick and Zeitz[77]
Chalk	0.1	Evison (in Vassil'ev and Gurevich[75])
Basalt	0.07	Levykin[79]

Very little information is available on the variation of shear wave attenuation with pressure or with depth in sediments and rocks. Gardner *et al.*[76] found that in unconsolidated (uncemented) sands, attenuation of shear and compressional waves varied about the same under increasing normal, effective pressures: attenuation decreased with about the $-\frac{1}{6}$ power of overburden pressure. Levykin[79] showed that both compressional-wave and shear-wave attenuation decreased about the same in low-porosity rocks under increasing effective pressure. There are no data on the effects of pressure on shear wave attenuation in unlithified, higher-porosity silt-clays.

In the absence of data, and in view of the work of

Gardner *et al.*, and Levykin, it can be assumed for modeling purposes that shear-wave attenuation varies with depth in the sea floor proportionally with compressional wave attenuation. Values of k_s at various depths in the first, thick sediment layer in a geoacoustic model can be derived from a simple proportion starting at the sediment surface: k_s at Sfc/k_p at $Sfc = k_s$ at depth$/k_p$ at depth. Values of k_s in lower rock layers can be assigned from the text table above.

L. Density and porosity

The values and variations of density and porosity at the surface and with depth in marine sediments and rocks are of importance in both basic and applied studies of the earth. Specifically (in the field of sound interactions with the sea floor), density of various layers of the oceanic crust are important in the propagation of shear and compressional waves, and other elastic waves. Values of density are required in all mathematical models of sound interacting with the sea floor. However, work at the Applied Research Laboratories of the University of Texas has indicated that, in many cases, the gradient of density may have only a small effect on bottom losses. At high grazing angles (above the shear-wave grazing angle), the effects amount to about 1–2 dB change in bottom loss. At low angles, very little effect is observed except in the vicinity of the low-angle shear anomaly where it can amount to as much as 2–8 dB (Hawker *et al.*,[43] p. 65).

The saturated bulk density at the surface of the sea floor, ρ_{sat}, in g/cm^3, can be computed from generalized, averaged coring data for the area using sediment-fractional porosity, n, the bottom-water density, ρ_w, and the bulk mineral grain density, ρ_s, in the equation

$$\rho_{sat} = n\rho_w + (1-n)\rho_s. \tag{10}$$

When cores are not available, porosities and densities can be predicted from tables (e.g., Tables I, II).

Two recent reports (Hamilton[10,54]) were concerned with *in situ* variations of density with depth in sea-floor sediments and rocks. The first report[10] was concerned with density as a function of depth in soft sediments in the sea floor. Based mainly on DSDP samples, generalized *in situ* profiles of porosity and density versus depth in the sea floor were constructed for some important sediment types: calcareous and siliceous oozes, pelagic clay, and terrigenous sediments.

The critical question in relating laboratory measurements of sediment density and porosity to *in situ* measurements in a deep borehole is: How much has the sample expanded elastically as a result of removal from overburden pressure in the borehole to atmospheric pressure in the laboratory? This was the problem addressed in Hamilton.[10] To construct *in situ* profiles, the results of consolidation tests were used to estimate the amount of elastic rebound (increase in volume) which has occurred after removal of the samples from overburden pressure in the boreholes. An example of the results of this procedure are illustrated in Fig. 21. The laboratory measurements of porosity were obtained from samples from DSDP Site 222 in the Arabian Sea

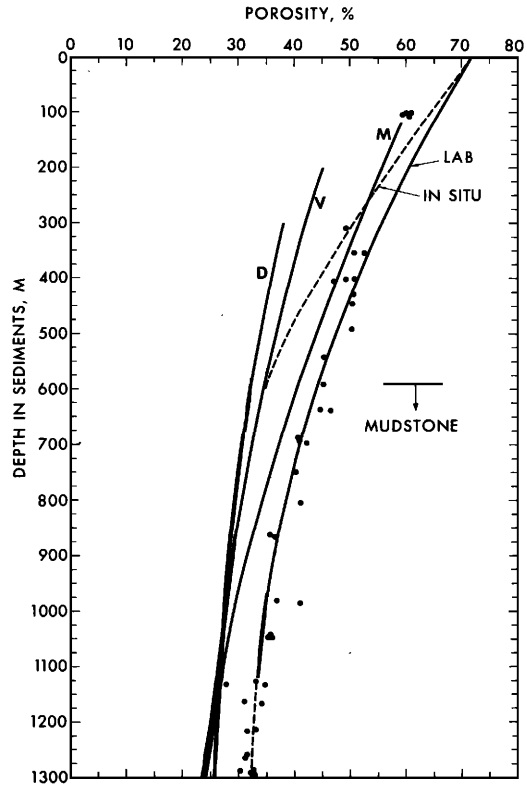

FIG. 21. Sediment and rock porosity versus depth in terrigenous sediments and rocks of the sea floor. Dots—laboratory measurements on samples from DSDP Site 222 in the Arabian Sea. The *in situ* curve is discussed at length in Hamilton[10] and briefly discussed in the text. Curve "D"—Gulf Coast shale (Dickinson[96]); curve "V"—shale from Vassoevich (in Rieke and Chilingarian,[97] p. 40); curve "M"—mudstone in Japan (Magara[26]).

(Bachman and Hamilton[85]). At this site, there was an unusually thick section of homogeneous, terrigeneous sediment which was drilled to about 1300 m. The amounts of estimated elastic rebound (from curves of depth and pressure versus rebound) were subtracted from the laboratory measurements to establish the *in situ* curve. This curve was joined at about 600 m to porosity-depth curves for shale and mudstone from the literature. In the various sediment types discussed in the 1976 report,[10] there is less reduction of porosity with depth in the first 100 m in these deep-water sediments than previously supposed: 8%–9% in pelagic clay, and calcareous and terrigenous sediments, and only 4%–5% in siliceous sediments.

After establishment of an *in situ* porosity-depth curve, a density-depth curve can be easily computed. Figure 22 illustrates the results for the various sediment types. The type of information in the 1976 report[10] can be helpful in predicting general density and porosity values for the sediment surface and for density gradients in the upper parts of the first layers of various sediment types.

Continuous acoustic reflection surveys are rapidly delineating the sediment and rock layers of the sea floor. Wide-angle reflection and refraction measurements (as with expendable sonobuoys) yield velocities in these layers. This allows true thicknesses to be

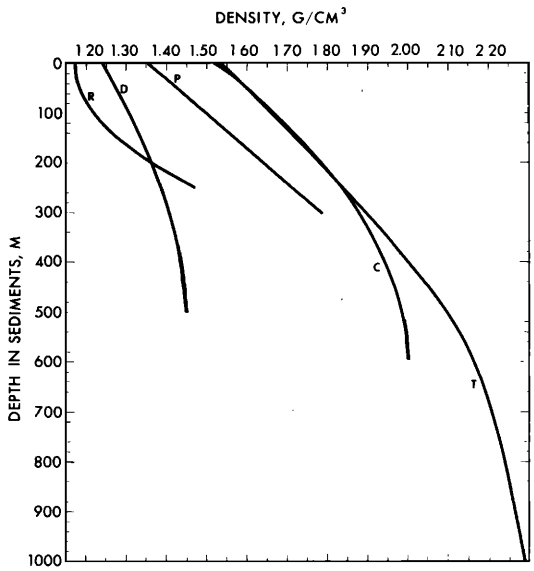

FIG. 22. *In situ* density of various marine sediments versus depth in the sea floor. Letters indicate sediment type: R is radiolarian ooze; D is diatomaceous ooze; P is pelagic clay; C is calcareous sediment; T is terrigenous sediment. Densities were computed from *in situ* porosities (see Hamilton[10] for discussions).

computed. Further, the new velocity data can frequently be linked to sediment and rock types by geologic reasoning, and by direct linkage to the boreholes of the Deep Sea Drilling Project. Therefore, it would be useful to establish relationships between velocity and density in the various sediment and rock types in the sea floor. This would allow prediction of density (a prime requirement) and density gradients to correspond to measured sound velocities for purposes of modeling the sea floor for underwater acoustics and geophysical studies.

Measurements of density and velocity in marine sediments at the Naval Ocean Systems Center were combined with information from the literature and a report published (Hamilton[54]) which relates density and velocity for common sediments and rocks. In the past, single curves of velocity versus density represented all sediment and rock types. The new data allow construction of separate velocity–density curves for the principal marine sediment and rock types. Carefully selected data from the laboratory and *in situ* measurements were used to present empirical sound velocity–density relations (in the form of regression curves and equations) in terrigenous silt clays, turbidites, and shale (Fig. 23), in calcareous materials (sediments, chalk, and limestone; Fig. 24), and in siliceous materials (sediments, porcelanite, and chert; Fig. 25). Figure 13 illustrates density–porosity relationships in DSDP basalts. Speculative curves were presented for composite sections of basalt and sediments (Hamilton,[54] Fig. 5).

It can be seen from the collection of curves (Fig. 26) that both the Nafe and Drake curve (labeled "ND"), in Ludwig *et al.*,[86] and the Gardner *et al.*,[87] curve (labeled "G"), are good generalizations of the velocity–density relations in the sea floor. This is especially notable

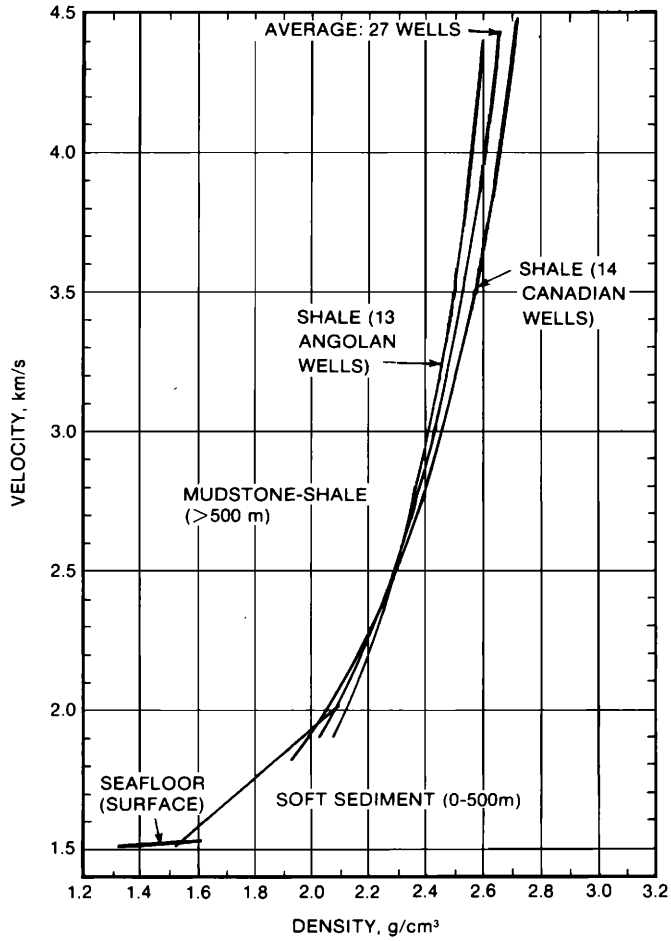

FIG. 23. Compressional wave velocity versus density in marine sediments (silt-clays, turbidites) and sedimentary rocks (mudstones, shales) from terrigenous sources. The curve for shale in Canadian wells is from Magara[26]; for shale from Angola: Perrier and Quiblier.[25] For regression equations and discussions see Hamilton.[54] *In situ* conditions are approximated.

in that most of the data used in the 1978 report[54] were not available to these authors, and the curve of Gardner *et al.*, was largely based on laboratory measurements of rocks from oil wells and *in situ* sonic and density well logs.

A frequently noted problem in geophysics has been that a given compressional wave velocity usually does not identify the rock type. This is apparent in Fig. 26, a composite of the curves of Figs. 23–25, plus the general curves of Nafe and Drake and Gardner *et al.* For example, at a velocity of 4.0 km/s the rock type could be any of those whose curves are illustrated. At 5.0 km/s only terrigenous rock (mudstone, shale) has been eliminated. However, the results of the DSDP, and reflection records, can be used in many areas to help select the appropriate rock type, and thus the appropriate velocity–density curve. In this way a better value of density can be determined for a given velocity.

ACKNOWLEDGMENTS

This work was supported by the Naval Electronic Systems Command (Code 320), by the Naval Sea Sys-

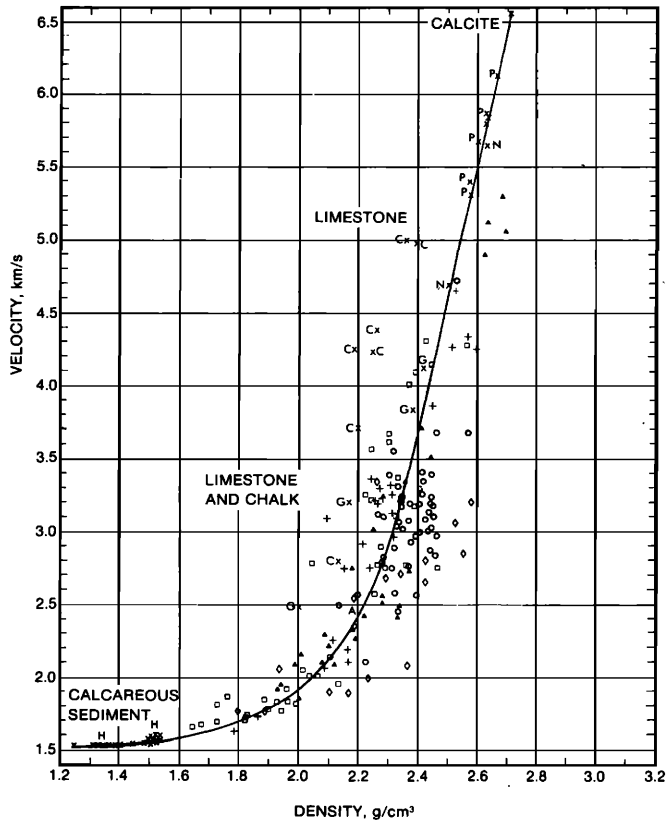

FIG. 24. Compressional wave velocity versus density in marine calcareous sediments and rocks. The letters indicate data from references (see Hamilton[54] for references, regression equations, and discussions). *In situ* conditions are approximated.

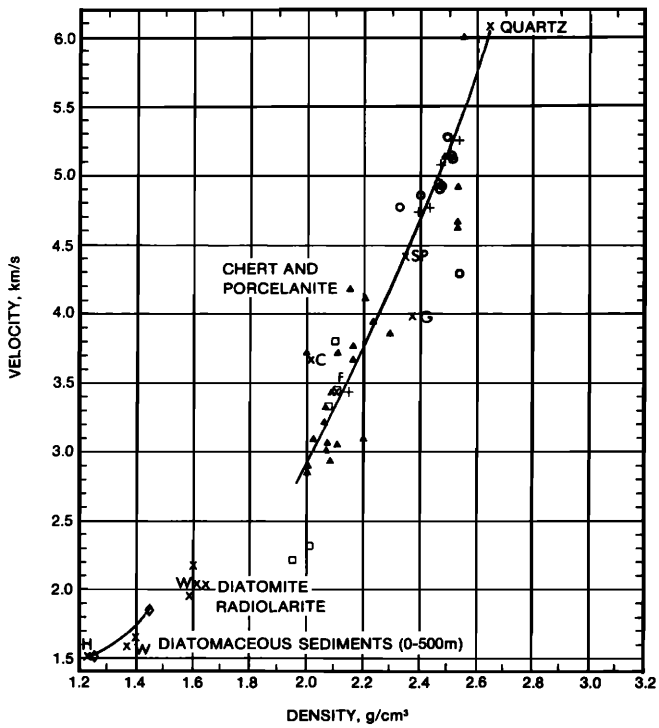

FIG. 25. Compressional wave velocity versus density in marine siliceous sediments and rocks. The letters indicate data from references. *In situ* conditions are approximated. See Hamilton[54] for discussions, references, and regression equations.

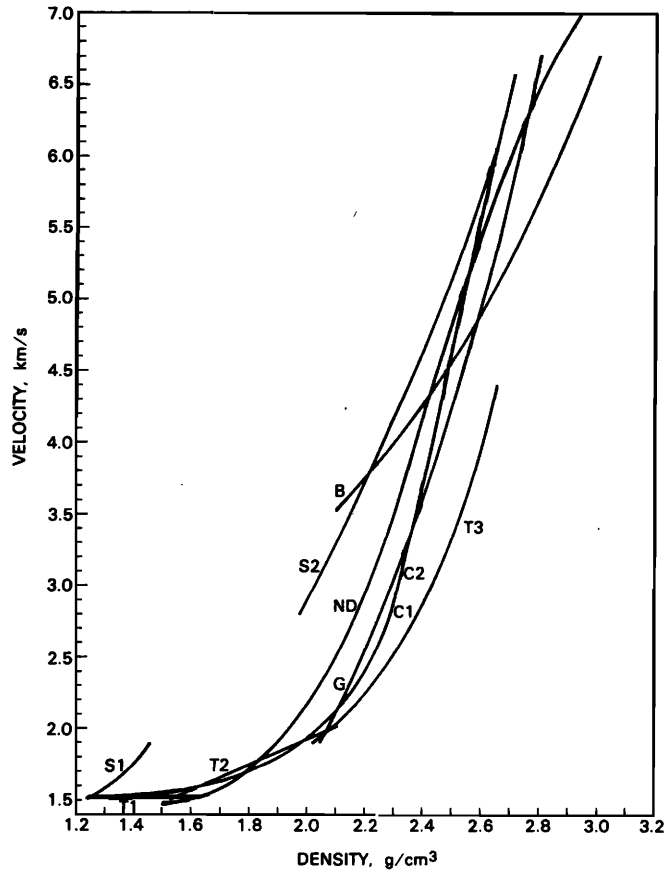

FIG. 26. A summary of compressional wave velocity versus density in various sediment and rock types of the sea floor, plus general curves from the literature. The letters beside the curves denote the sediment or rock types: S1—diatomaceous sediments (0–500 m); S2—siliceous rocks; T1—terrigenous surface sediments; T2—turbidites (0–500 m); T3—mudstones, shales; C1—chalk, limestone; C2—limestone; B—basalt. The general curves of Nafe and Drake[86] (labeled *ND*) and Gardner *et al.*[87] (labeled G) are included for comparisons. See Hamilton[54] for references, discussions, and regression equations.

tems Command (Code 06H1), and by the Office of Naval Research.

APPENDIX A: AN EXAMPLE OF A GEOACOUSTIC MODEL

1. Introduction

A geoacoustic model can be presented in many ways The correct form should be selected for most utility to the user. For purposes of underwater acoustics, the writer has used several forms. One was illustrated and discussed in Hamilton.[2] The most recent form is illustrated in this Appendix. The geoacoustic model is for an actual area in which acoustic experiments were made. The methods used to derive the values are discussed under appropriate headings in the main text. As noted and discussed in the text, a geoacoustic model of this type should be accompanied by a best-available bathymetric chart, echosounder and acoustic reflection records, oceanographic cast data, and sufficient information from the literature (especially from the Deep Sea Drilling Project) to allow extrapolation of the geo-

logical, geophysical, and acoustic data within geomorphic provinces of the sea floor.

2. An example model

a. Location, water depth, and description of the sea floor

Tabulated material (Tables VIA and VIB) are preceded by the following information: (1) Geoacoustic Model No. (2) General area. (3) Location (lat, long). (4) Water depth, echo-sounder depth, and corrected (true) depth; in this case the true depth is 5100 m. (5) Geomorphic province and description of the sea floor. In this case the area is in the Abyssal Plain Province (the description of the sea floor is here omitted).

b. Descriptive material to accompany Table VIA

(1) V_p (compressional wave (sound) velocity).

(a) First layer (from sonobuoy measurements).

$V_p = 1.528 + 1.25D - 0.45D^2 + 0.0568D^3$, where V_p is in km/s, and depth in the sea floor, D, is in km.

(b) Lower layers: V_ps from literature.

(2) V_s (shear wave velocity). From a study by Hamilton[47] of V_p/V_s ratios in marine sediments and rocks. Basalt V_s from Christensen and Salisbury.[49]

(3) k_p (Constant in: attenuation of compressional waves, α_p, in dB/m $= k_p f$; where f is frequency in kHz). The three listed values to 300 m are: probable minimum, recommended for first trial in bottom-loss modeling, and probable maximum. From Hamilton.[2,55,56]

(4) k_s (Constant in: attenuation of shear waves, α_s, in dB/m $= k_s f$; where f is frequency in kHz. Based on Hamilton[81] at surface; proportional to k_p at depth.

(5) Density (Saturated bulk density, *in situ*). Surface density computed from core data. Density at depth from Hamilton.[10,54] Basalt density from Christensen and Salisbury.[49]

(6) General

(a) "Thickness, s" (in seconds of one-way sound travel time) from reflection records. "Thickness,

TABLE VIA. An example of the main table for a geoacoustic model, showing properties of the sediment and rock layers plus sound speed and density of the water just above the sea floor (bottom water).

Layer material / Layer no.	Thickness (s)	Thickness (m)	Depth (m)	Velocity (m/s) V_p	Velocity (m/s) V_s	Attenuation k_p			Attenuation k_s	Density (g/cm^3)
Bottom water	(See Note 6c)			1543.8						1.050 65
Sea Floor										
Sediment			Sfc	1528	125	0.04	0.08	0.18	15.0	1.42
			100	1649	390	0.06	0.09	0.17	19.3	1.68
			200	1760	448	0.09	0.11	0.16	23.5	1.81
			300	1864	507	0.11	0.12	0.15	25.7	1.93
and			400	1960	570		0.14		30.0	2.03
			500	2048	636		0.14		30.0	2.11
1 Sedimentary	0.76	1580	600	2128	702		0.12		25.7	2.14
			700	2202	755		0.11		23.5	2.17
rock			800	2269	810		0.10		21.4	2.19
			900	2330	855		0.08		17.1	2.22
			1000	2385	900		0.07		15.0	2.24
			1500	2582	1050		0.04		8.6	2.30
			1595–	2607	1070		0.03		6.4	2.31
			1595+	3500	1750		0.03		3.0	2.54
2 Sedimentary rock	0.25	940	2065	3750	1875		0.02		3.0	2.58
			2535–	4000	2000		0.02		3.0	2.61
3 Basalt			2535+	5300	2680		0.02		0.07	2.70

TABLE VIB. Detailed properties of the top three meters of the first sediment layer in Table VIA.

Layer no.	Material	Depth (m)	Velocity (m/s) V_p	Velocity (m/s) V_s	Attenuation k_p			Attenuation k_s	Density (g/cm^3)
	Bottom water		1543.8						1.050 65
Sea floor									
1a	Silt-clay	*Sfc*	1513	115	0.03	0.07	0.17	15.0	1.39
		2.8–	1517	128	0.03	0.07	0.17	15.0	1.39
1b	Sand-silt-clay	2.8+ 3.0–	1635	175	0.45	0.65	0.85	13.0	1.78

m" from one-way travel time and layer mean velocity.

(b) In the above model, the "*Sfc*" values are a composite for the 0–3 m depth interval. For a detailed model of this interval see Table VIB.

(c) *In situ* properties of the bottom water:

True depth: 5100 m
Temperature: 1.38 °C
Salinity: 34.69 *ppt*
Pressure: 529.6 kg/cm^2
Sound speed: 1543.8 m/s
Density: 1.050 65 g/cm^3
Impedance: 1.621 99 g/cm^{2}s$\times 10^5$

c. Descriptive material to accompany Table VIB

(1) The geoacoustic models (such as in the main table) showing thick sediment and sedimentary rock sections over "acoustic basement" (such as basalt) are generalized and do not account for the multiple reflectors as seen (usually at high frequencies), for example in the 3.5 kHz records, or in cores.

(2) If a detailed, multireflector model is desired, the above sequence (Table VIB) of a thicker silt-clay layer and a thinner silt (or other) layer, can be alternated to any desired depth, with random variations in layer thicknesses. If so, the property values can be corrected for depth as follows.

(a) For the silt-clay layer

(i) For V_p: Increase V_p using gradients computed from the V_p versus depth equation.

(ii) Other properties: Vary the value of the property with depth using the appropriate gradient from the values listed in the main table.

(b) For the sand-silt-clay layer

(i) For V_p: Increase V_p as above for silt-clay.
(ii) For k_p: Vary k_p along line "B" and "C" (Fig. 20).
(iii) Other properties: as above for silt-clay.

(3) It should be noted that in areas where turbidites form abyssal plains or fans (such as in the Gulf of Alaska, Bengal Fan, or western Atlantic) the reflectors usually represent coarser sediments spilling discontinuously from leveed channels. These reflectors cannot, usually, be followed over very great distances, nor correlated from area to area. Any detail, as above, is a gross generalization of widely varying layers (in thickness and properties).

(4) The values listed in the main, general table for "*Sfc*" are composite values for the 0–3 m depth interval (Table VIB). Some averaged properties in four cores for this interval, other than those listed above, are as follows [porosity in silt-clay (0–100 cm) is salt corrected; porosity in sand-silt-clay based on velocity-porosity relations from other data].

Property	Silt clay	Sand-silt-clay
Velocity ratio	0.98	1.06
	Composite: 0.99	
Porosity, %	79.00	55
	Composite: 77	
Mean grain size, ϕ	8.95	5.48
(No. in sample)	(182)	(2)
Grain density, g/cm^3	Avg. all samples	2.66
(No. in sample)		(179)

(5) Although the generalized illustration, above, indicates a sharp top boundary between the silt-clay and sand-silt-clay layer, it is more apt to be gradational in all properties.

APPENDIX B: ELASTIC AND VISCOELASTIC MODELS FOR MARINE SEDIMENTS

1. Introduction

Although not usually a part of a final geoacoustic model, the modeler should understand the interrelationships between the elastic and viscoelastic constants with which he is working. Some computations require this knowledge, especially when recomputing data from the literature.

In earlier literature various elastic and viscoelastic models have been applied to water-saturated sediments (e.g., Hookean, Kelvin–Voigt, Maxwell). These and associated subjects have been reviewed by the writer in previous reports.[2,3,29,55,81,88] The following viscoelastic model was selected to best represent water-saturated, natural marine sediments. The only other presently viable model is that of Biot[68,69] as refined by Stoll and Bryan,[60] by Stoll,[61-63] by Hovem,[70] and by Hovem and Ingram.[71] These two models are not necessarily in conflict at all points; especially in view of the fact that the viscoelastic model favored below, does not specify the mechanics of attenuation of compressional and shear waves. Some aspects of these models have been discussed in the sections on attenuation in the main text. Stoll will elaborate his thoughts on these subjects in the present series of papers.

2. A viscoelastic model for marine sediments

The subject of elastic and viscoelastic models for water-saturated sediments was recently reviewed (references above), and a particular viscoelastic model was favored. For an extended discussion with appropriate references, the reader is referred to these reports. In general, it was assumed that most marine sediments have a macroscopically isotropic, two-phase system (water and minerals). The compressional and shear waves passing through this system are small sinusoidal stresses which cause strains less than about 10^{-5} or 10^{-6}, with wavelengths much greater than grain sizes. Frequencies are from about one Hz to the MHz range. It was further noted that almost no marine sediments can be considered suspensions, and that almost all have structures with sufficient rigidity to transmit shear waves. Other restrictive parameters are noted below.

The mathematical model outlined in this section has several advantages. It does not specify the mechanics of attenuation, and includes provision for velocity dispersion and nonlinear dependence of attenuation on frequency. The user is thus not committed, *a priori*, to no-velocity dispersion, or to any particular relationship between attenuation and frequency. The model indicates clearly those factors involving velocity dispersion and nonlinear attenuation which, if negligible, can be dropped. It indicates clearly under what conditions Hookean elastic equations can be used to interrelate wave velocities and other elastic moduli. And interestingly, this model has been widely used in studies of rocks and the earth's crust, as well as in the properties of polymers, and in some soil mechanics studies.

The favored model is a case of linear viscoelasticity in which the Lamé elastic moduli μ and λ are replaced by complex moduli, $(\mu + i\mu')$ and $(\lambda + i\lambda')$, in which μ, λ, and density govern wave velocity and the imaginary moduli, $i\mu'$ and $i\lambda'$ govern energy damping.

The basic derivations of the above model are in Ferry[89] and White,[90] and will not be repeated here; the final equations repeated below are from Hamilton.[55] Without assumptions as to negligible factors, the equations of the model in the form of Bucker (in Hamilton *et al.*,[88] p. 4046; or in Ferry,[89] pp. 94 and 419), reduce to the following for both compressional and shear waves (with some changes in notation):

$$\frac{1}{Q} = \frac{aV}{\pi f - a^2V^2/4\pi f}, \tag{B1}$$

where

$1/Q$ is the specific attenuation factor, or specific dissipation function,

a is the attenuation coefficient,

V is wave velocity,

f is frequency (circular frequency, $\omega = 2\pi f$).

Subscripts (p or s) can be inserted into Eq. (B1) when referring to compressional or shear waves.

When energy damping is small [i.e., $\lambda' \ll \lambda$ and $\mu' \ll \mu$ (White,[90] p. 95), or (Ferry,[89] p. 123) $r \ll 1$, where $r = aV/2\pi f$], the right-hand term in the denominator of Eq. (B1), $a^2V^2/4\pi f$, is negligible and can be dropped. This leaves the more familiar expressions (e.g., Knopoff and Macdonald[91]; White[90]; Bradley and Fort[92]; Attwell and Ramana[93]):

$$1/Q = aV/\pi f, \tag{B2}$$

$$1/Q = 2aV/\omega = \Delta/\pi = \tan\phi \tag{B3}$$

$$\Delta = aV/f, \text{ or } a = \Delta f/V. \tag{B4}$$

Additionally

$$1/Q_p = \tan\phi_p = (\lambda' + 2\mu')/(\lambda + 2\mu), \tag{B5}$$

$$1/Q_s = \tan\phi_s = \mu'/\mu, \tag{B6}$$

$$\Delta E/E = 2\pi/Q, \tag{B7}$$

$$\alpha = 8.686a, \tag{B8}$$

where (in addition to those symbols already defined)

Δ is the logarithmic decrement (natural log of the ratio of two successsive amplitudes in an exponentially decaying sinusoidal wave),

$\tan\phi$ is the loss angle

$\Delta E/E$ is the fraction of strain energy lost per stress cycle,

α is attenuation in dB/linear measure (e.g., dB/cm).

Equations involving compressional and shear-wave velocities in Hamilton *et al.*,[88] or in Ferry,[89] are (in Ferry's notation):

$$(\lambda + 2\mu) = \rho V_p^2 (1 - r^2)/(1 + r^2)^2, \tag{B9}$$

$$\mu = \rho V_s^2 (1 - r^2)/(1 + r^2)^2 \tag{B10}$$

where $r = aV/2\pi f$, λ = Lamé's constant, μ = rigidity, ρ = density.

In Eqs. (B9) and (B10) the term, $(1 - r^2)/(1 + r^2)^2$, indicates the degree of velocity dispersion for linear viscoelastic media. When damping is small (defined above), this term is negligibly close to one and can be dropped, as implied by Ferry[89] (p. 94). This leaves the more familiar Hookean equations

$$(\lambda + 2\mu) = \rho V_p^2, \tag{B11}$$

$$\mu = \rho V_s^2. \tag{B12}$$

Computations with the data of Hamilton,[55] and with data from the literature, indicate that most water-saturated rocks and sediments qualify under the above definitions as media with "small damping." For example, computations from Table I, in Hamilton[55] indicate that the factor $(1 - r^2)/(1 + r^2)^2$ for compressional waves at 14 kHz is 0.9992 in fine sand, and an average of 0.9997 for four silty clays. In Pierre shale, the factor for shear waves is about 0.992.[59] Thus, the Hookean elastic equations, such as Eqs. (B11) and (B12), can be used to study low strain-wave velocities and elastic moduli in water-saturated sediments and rocks.

If the factor $(1 - r^2)/(1 + r^2)^2$ in Eqs. (B9) and (B10), and the term in the denominator of Eq. (B1), $a^2V^2/4\pi f$, are considered negligible and dropped, then wave velocities, $1/Q$, and the logarithmic decrement are independent of frequency, and linear attenuation is proportional to the first power of frequency.

Hamilton[2,55,56] summarized the evidence for velocity dispersion and relations between attenuation and frequency for compressional waves; some later information is in the main text of this report. It was concluded that from a few Hz to at least one MHz in silt-clays (mud), and from about one kHz to one MHz in sands, there was no measureable compressional velocity dispersion, linear attenuation was approximately related to the first power of frequency, and the logarithmic decrement and $1/Q$ were independent of frequency. If so, the same would be true for shear waves, and Eqs. (B2) through (B8), as well as (B11) and (B12) should apply to low-strain compressional and shear waves in water-saturated sediments and rocks. As noted in the

main text, recent studies and experiments by Stoll[62,63] agree with the above for muds, but Stoll and Hovem and Ingram[71] indicate velocity dispersion and nonlinear relationships between compressional and shear-wave attenuation and frequency in uniform-sized sands of high permeability.

[1]E. L. Hamilton, "Prediction of Deep-Sea Sediment Properties: State of the Art," in *Deep-Sea Sediments, Physical and Mechanical Properties*, edited by A. L. Inderbitzen (Plenum, New York, 1974), pp. 1–43.

[2]E. L. Hamilton, "Geoacoustic Models of the Sea Floor," in *Physics of Sound in Marine Sediments*, edited by L. Hampton (Plenum, New York, 1974), pp. 181–221.

[3]E. L. Hamilton, "Prediction of In Situ Acoustic and Elastic Properties of Marine Sediments," Geophysics **36**, 266–284 (1971).

[4]H. W. Menard, *Marine Geology of the Pacific* (McGraw–Hill, New York, 1964).

[5]F. P. Shepard, *Submarine Geology* (Harper and Row, New York, 1973), 3rd ed.

[6]F. P. Shepard, "Nomenclature Based on Sand-Silt-Clay Ratios," J. Sediment. Petrol. **24**, 151–158 (1954).

[7]NAVOCEANO, *Handbook of Oceanographic Tables*, Spcl. Publ. 68 (U. S. Naval Ocean. Office, Washington, DC, 1966).

[8]B. E. Tucholke and D. J. Shirley, "Comparison of Laboratory and In situ Compressional Wave Velocity Measurements on Sediment Cores from the Western North Atlantic," J. Geophys. Res. **84**, 687–695 (1979).

[9]E. L. Hamilton, "Sound Velocity and Related Properties of Marine Sediments, North Pacific," J. Geophys. Res. **75**, 4423–4446 (1970).

[10]E. L. Hamilton, "Variations of Density and Porosity with Depth in Deep-Sea Sediments," J. Sediment. Pet. **46**, 280–300 (1976).

[11]R. Houtz, J. Ewing, and X. LePichon, "Velocity of Deep-Sea Sediments from Sonobuoy Data," J. Geophys. Res. **73**, 2615–2641 (1968).

[12]R. Houtz, J. Ewing, and P. Buhl, "Seismic Data from Sonobuoy Stations in the Northern and Equatorial Pacific," J. Geophys. Res. **75**, 5093–5111 (1970).

[13]E. L. Hamilton, D. G. Moore, E. C. Buffington, P. L. Sherrer, and J. R. Curray, "Sediment Velocities from Sonobuoys: Bay of Bengal, Bering Sea, Japan Sea, and North Pacific," J. Geophys. Res. **79**, 2653–2668 (1974).

[14]E. L. Hamilton, R. T. Bachman, J. R. Curray, and D. G. Moore, "Sediment Velocities from Sonobuoys: Bengal Fan, Sunda Trench, Andaman Basin, and Nicobar Fan," J. Geophys. Res. **82**, 3003–3012 (1977).

[15]R. E. Houtz, "Preliminary Study of Global Sediment Sound Velocities from Sonobuoy Data," in *Physics of Sound in Marine Sediments*, edited by L. Hampton (Plenum, New York, 1974), pp. 519–535.

[16]C. S. Clay and P. A. Rona, "Studies of Seismic Reflections from Thin Layers on the Ocean Bottom in the Western North Atlantic," J. Geophys. Res. **70**, 855–869 (1965).

[17]X. LePichon, J. Ewing, and R. E. Houtz, "Deep-Sea Sediment Velocity Determination Made While Reflection Profiling," J. Geophys. Res. **73**, 2597–2614 (1968).

[18]S. T. Knott and H. Hoskins, *Collection and Analysis of Seismic Wide Angle Reflection and Refraction Data Using Radio Sonobuoys*, Tech. Rept. 75–33 (Woods Hole Ocean. Inst., Woods Hole, MA, 1975).

[19]J. Schlee, J. C. Behrendt, J. A. Grow, J. M. Robb, R. E. Mattick, P. T. Taylor, and B. J. Lawson, "Regional Geologic Framework off Northeastern United States," Am. Assoc. Pet. Geol. Bull. **60**, 926–951 (1976).

[20]M. T. Taner and F. Koehler, "Velocity Spectra-Digital Computer Derivation and Applications of Velocity Functions," Geophysics **34**, 859–881 (1969).

[21]E. L. Hamilton, "Sound Velocity Gradients in Marine Sediments," J. Acoust. Soc. Am. **65**, 909–922 (1979).

[22]R. E. Houtz and J. I. Ewing, "Sedimentary Velocities of the Western North Atlantic Margin," Bull. Seismol. Soc. Am. **54**, 867–895 (1964).

[23]E. L. Hamilton, "Sound Speed and Related Properties of Sediments from Experimental Mohole (Guadalupe Site)," Geophysics **30**, 257–261 (1965).

[24]J. C. Fry and R. W. Raitt, "Sound Velocities at the Surface of Deep Sea Sediments," J. Geophys. Res. **66**, 589–597 (1961).

[25]R. Perrier and J. Quiblier, "Thickness Changes in Sedimentary Layers During Compaction History; Methods for Quantitative Evaluation," Am. Assoc. Petrol. Geol. Bull. **58**, 507–520 (1974).

[26]K. Magara, "Compaction and Migration of Fluids in Miocene Mudstone, Nagaoka Plain, Japan," Am. Assoc. Petrol. Geol. Bull. **52**, 2466–2501 (1968).

[27]B. Naini and M. Talwani, "Sediment Distribution and Structure in the Indus Cone and the Western Continental Margin of India (Arabian Sea)," Trans. Am. Geophys. Union **58**, 405(A) (1977).

[28]R. S. White and K. Klitgord, "Sediment Deformation and Plate Tectonics in the Gulf of Oman," Earth Planet. Sci. Lett. **32**, 199–209 (1976).

[29]E. L. Hamilton, "Elastic Properties of Marine Sediments," J. Geophys. Res. **76**, 579–604 (1971).

[30]E. L. Hamilton, "Shear Wave Velocity versus Depth in Marine Sediments: A Review," Geophysics **41**, 985–996 (1976).

[31]H. E. Morris, "Bottom-Reflection-Loss Model with a Velocity Gradient," J. Acoust. Soc. Am. **48**, 1198–1202 (1970).

[32]J. S. Hanna, "Short-Range Transmission Loss and the Evidence for Bottom-Refracted Energy," J. Acoust. Soc. Am. **53**, 1686–1690 (1973).

[33]R. E. Christensen, J. A. Frank, and W. H. Geddes, "Low-Frequency Propagation via Shallow Refracted Paths Through Deep Ocean Unconsolidated Sediments," J. Acoust. Soc. Am. **57**, 1421–1426 (1975).

[34]D. C. Stickler, "Negative Bottom Loss, Critical-Angle Shift, and the Interpretation of the Bottom Reflection Coefficient," J. Acoust. Soc. Am. **61**, 707–710 (1977).

[35]K. E. Hawker, K. C. Focke, and A. L. Anderson, *A Sensitivity Study of Underwater Sound Propagation Loss and Bottom Loss*, ARL-TR-77-17 (Applied Res. Labs., Univ. of Texas, Austin, 1977).

[36]J. I. Ewing and J. E. Nafe, "The Unconsolidated Sediments," in *The Sea, Vol. 3: The Earth Beneath the Sea*, edited by M. N. Hill (Interscience, New York, 1963), pp. 73–84.

[37]R. E. Houtz and J. I. Ewing, "Detailed Sedimentary Velocities from Seismic Refraction Profiles in the Western North Atlantic," J. Geophys. Res. **68**, 5233–5258 (1963).

[38]S. O. Schlanger and R. G. Douglas, "The Pelagic Ooze-Chalk-Limestone Transition and its Implications for Marine Stratigraphy," in *Pelagic Sediments on Land and under the Sea*, edited by K. J. Hsü and H. C. Jenkyns, Spec. Publ. No. 1, Int. Assoc. Sedimentologists (Blackwell, London, 1974), pp. 117–148.

[39]T. C. Johnson, E. L. Hamilton, R. T. Bachman, and W. H. Berger, "Sound Velocities in Calcareous Oozes and Chalks from Sonobuoy Data: Ontong–Java Plateau, Western Equatorial Pacific," J. Geophys. Res. **83**, 283–288 (1978).

[40]E. L. Hamilton, "Sound Channels in Surficial Marine Sediments," J. Acoust. Soc. Am. **48**, 1296–1298 (1970).

[41]H. P. Bucker and H. E. Morris, "Reflection of Sound from a Layered Ocean Bottom," in *Proceedings of a Conference on Oceanic Acoustic Modelling*, SACLANTCEN Conf. Proc. No. 17, edited by W. Bachmann and R. B. Williams (SACLANT ASW Res. Centre, La Spezia, Italy, 1975), pp. 19–35.

[42]K. E. Hawker and T. L. Foreman, *A Plane Wave Reflection Coefficient Model Based on Numerical Integration: Formula-*

tion, Implementation, and Application, ARL-TR-76-23 (Applied Res. Labs., Univ. of Texas, Austin, 1976).
[43]K. E. Hawker, A. L. Anderson, K. C. Focke, and T. L. Foreman, *Initial Phase of a Study of Bottom Interaction of Low Frequency Underwater Sound,* ARL-TR-76-14 (Applied Res. Labs., Univ. of Texas, Austin, 1976).
[44]K. E. Hawker, "The Influence of Stoneley Waves on Plane Wave Reflection Coefficients: Characteristics of Bottom Reflection Loss," J. Acoust. Soc. Am. **64**, 548–555 (1978).
[45]K. E. Hawker, "Existence of Stoneley Waves as a Loss Mechanism in Plane Wave Reflection Problem," J. Acoust. Soc. Am. **65**, 682–686 (1979).
[46]P. J. Vidmar and T. L. Foreman, "A Plane Wave Reflection Loss Model including Sediment Rigidity," J. Acoust. Soc. Am. **66**, 1830–1835 (1979).
[47]E. L. Hamilton, "V_p/V_s and Poisson's Ratios in Marine Sediments and Rocks," J. Acoust. Soc. Am. **66**, 1093–1101 (1979).
[48]Y. Ohta and N. Goto, "Empirical Shear Wave Velocity Equations in Terms of Characteristic Soil Indexes," Earthquake Eng. Struct. Dyna. **6**, 167–187 (1978).
[49]N. I. Christensen and M. H. Salisbury, "Structure and Constitution of the Lower Oceanic Crust," Rev. Geophys, Space Phys. **13**, 57–86 (1975).
[50]R. D. Hyndman and M. J. Drury, "The Physical Properties of Oceanic Basement Rocks from Deep Drilling on the Mid-Atlantic Ridge," J. Geophys. Res. **81**, 4042–4052 (1976).
[51]T. J. G. Francis, "The Ratio of Compressional to Shear Velocity and Rock Porosity on the Axis of the Mid-Atlantic Ridge," J. Geophys. Res. **81**, 4361–4364 (1976).
[52]M. Talwani, C. C. Windisch, and M. G. Langseth, "Reykjanes Ridge Crest: A Detailed Geophysical Study," J. Geophys. Res. **76**, 473–517 (1971).
[53]R. E. Houtz, "Seismic Properties of Layer 2A in the Pacific," J. Geophys. Res. **81**, 6321–6331 (1976).
[54]E. L. Hamilton, "Sound Velocity-Density Relations in Sea-Floor Sediments and Rocks," J. Acoust. Soc. Am. **63**, 366–377 (1978).
[55]E. L. Hamilton, "Compressional Wave Attenuation in Marine Sediments," Geophysics **37**, 620–646 (1972).
[56]E. L. Hamilton, "Sound Attenuation as a Function of Depth in the Sea Floor," J. Acoust. Soc. Am. **59**, 528–535 (1976).
[57]L. Bjorno, "Finite-Amplitude Wave Propagation through Water-Saturated Marine Sediments," Acustica **38**, 195–200 (1977).
[58]K. Kudo and E. Shima, "Attenuation of Shear Waves in Soil," Bull. Earthquake Res. Inst., Univ. Tokyo **48**, 145–158 (1970).
[59]F. J. McDonal, F. A. Angona, R. L. Mills, R. L. Sengbush, R. G. Van Nostrand, and J. E. White, "Attenuation of Shear and Compressional Waves in Pierre Shale," Geophysics **23**, 421–439 (1958).
[60]R. D. Stoll and G. M. Bryan, "Wave Attenuation in Saturated Sediments," J. Acoust. Soc. Am. **47**, 1440–1447 (1970).
[61]R. D. Stoll, "Acoustic Waves in Saturated Sediments," in *Physics of Sound in Marine Sediments,* edited by L. Hampton (Plenum, New York, 1974), pp. 19–39.
[62]R. D. Stoll, "Acoustic Waves in Ocean Sediments," Geophysics **42**, 715–725 (1977).
[63]R. D. Stoll, "Experimental Studies of Attenuation in Sediments," J. Acoust. Soc. Am. **64**, 5143(A) (1978).
[64]F. N. Tullos and C. Reid, "Seismic Attenuation of Gulf Coast Sediments," Geophysics **34**, 516–528 (1969).
[65]Yu. P. Neprochnov, "Seismic Studies of the Crustal Structure beneath the Seas and Oceans," Oceanology (English trans.) **11**, 709–715 (1971).
[66]E. G. McLeroy and A. De Loach, "Sound Speed and Attenuation, from 15 to 1500 kHz, Measured in Natural Sea Floor Sediments," J. Acoust. Soc. Am. **44**, 1148–1150 (1968).
[67]C. McCann and D. M. McCann, "The Attenuation of Compressional Waves in Marine Sediments," Geophysics **34**, 882–892 (1969).
[68]M. A. Biot, "Theory of Propagation of Elastic Waves in a Fluid-Saturated Porous Solid. I. Low-Frequency Range," J. Acoust. Soc. Am. **28**, 168–178 (1956).
[69]M. A. Biot, "Theory of Propagation of Elastic Waves in a Fluid-Saturated Porous Solid. II. Higher-Frequency Range," J. Acoust. Soc. Am. **28**, 179–191 (1956).
[70]J. M. Hovem, "The Nonlinearity Parameter of Saturated Marine Sediments," J. Acoust. Soc. Am. **66**, 1463–1467 (1979).
[71]J. M. Hovem and G. D. Ingram, "Viscous Attenuation of Sound in Saturated Sand," J. Acoust. Soc. Am. **66**, 1807–1812 (1979).
[72]D. W. Bell, *Shear Wave Propagation in Unconsolidated Fluid Saturated Porous Media,* ARL-TR-79-31 (Applied Res. Labs., Univ. of Texas, Austin, 1979).
[73]R. C. Tyce, "Near-Bottom Observations of Sea-Floor Acoustics," Ph.D. dissertation, University of California, San Diego (1977).
[74]R. E. Sheriff, "Factors Affecting Seismic Amplitudes," Geophys. Prospecting **23**, 125–138 (1975).
[75]Y. L. Vassil'ev and G. L. Gurevich, "On the Ratio between Attenuation Decrements and Propagation Velocities of Longitudinal and Transverse Waves," Bull. Acad. Sci. USSR Ser. Geophys. (English transl.) No. 12, 1061–1074 (1962).
[76]G. H. F. Gardner, M. R. J. Wyllie, and D. M. Droschak, "Effects of Pressure and Fluid Saturation on the Attenuation of Elastic Waves in Sands," J. Pet. Technol. **16**, 189–198 (1964).
[77]L. Peselnick and I. Zietz, "Internal Friction of Fine-Grained Limestones at Ultrasonic Frequencies," Geophysics **24**, 285–296 (1959).
[78]S. Balakrishna and Y. V. Ramana, "Integrated Studies of the Elastic Properties of some Indian Rocks," in *The Crust and Upper Mantle of the Pacific Area,* edited by L. Knopoff, C. L. Drake, and P. J. Hart, Geophys. Mon. No. 12 (Am. Geophys. Union, Washington, DC, 1968), pp. 489–500.
[79]A. I. Levykin, "Longitudinal and Transverse Wave Absorption and Velocity in Rock Specimens at Multilateral Pressures up to 4000 kg/cm^2," Bull. Acad. Sci. USSR Phys. Solid Earth (English transl.) No. 2, 94–98 (1965).
[80]Yu. P. Neprochnov, A. F. Neprochnova, S. M. Zverev, and V. I. Mironova, "Deep Seismic Sounding of the Earth's Crust in the Central Part of the Black Sea Depression," in *Problems in Deep Seismic Sounding,* edited by S. M. Zverev (English translation, Consultant's Bureau, New York, 1967), pp. 49–78.
[81]E. L. Hamilton, "Attenuation of Shear Waves in Marine Sediments," J. Acoust. Soc. Am. **60**, 334–338 (1976).
[82]R. Meissner, "*P*- and *SV*-Waves from Uphole Shooting," Geophysical Prospecting **13**, 433–459 (1965).
[83]R. E. Warrick, "Seismic Investigation of a San Francisco Bay Mud Site," Bull. Seismol. Soc. Am. **64**, 375–385 (1974).
[84]L. V. Molotova, "Velocity Dispersion of Body Waves in Terrigenous Rocks," Bull. Acad. Sci. USSR Phys. Solid Earth (English transl.) No. 7, 500–506 (1966).
[85]R. T. Bachman and E. L. Hamilton, "Density, Porosity, and Grain Density of Samples from Deep Sea Drilling Project Site 222 (Leg 23) in the Arabian Sea," J. Sediment. Petrol. **46**, 654–658 (1976).
[86]W. J. Ludwig, J. E. Nafe, and C. L. Drake, "Seismic Refraction," in *The Sea, Vol. 4, Pt. 1,* edited by A. E. Maxwell (Wiley, New York, 1970), pp. 53–84.
[87]G. H. F. Gardner, L. W. Gardner, and A. R. Gregory, "Formation Velocity and Density-The Diagnostic Basics for Stratigraphic Traps," Geophysics **39**, 770–780 (1974).
[88]E. L. Hamilton, H. P. Bucker, D. L. Keir, and J. A. Whitney, "Velocities of Compressional and Shear Waves in Marine Sediments Determined In Situ from a Research Submersible," J. Geophys. Res. **75**, 4039–4049 (1970).
[89]J. D. Ferry, *Viscoelastic Properties of Polymers* (Wiley, New York, 1961).
[90]J. E. White, *Seismic Waves: Radiation, Transmission, and Attenuation* (McGraw-Hill, New York, 1965).

[91]L. Knopoff and G. J. F. MacDonald, "Attenuation of Small Amplitude Stress Waves in Solids," Rev. Mod. Phys. **30**, 1178–1192 (1958).
[92]J. J. Bradley and A. N. Fort, Jr., "Internal Friction in Rocks," in *Handbook of Physical Constants*, edited by S. P. Clark, Jr., Mem. No. 97 (Geol. Soc. Am., New York, 1966), pp. 175–194.
[93]P. B. Attwell and Y. V. Ramana, "Wave Attenuation and Internal Friction as Functions of Frequency in Rocks," Geophysics **31**, 1049–1056 (1966).
[94]R. L. Geyer and S. T. Martner, "SH Waves from Explosive Sources," Geophysics **34**, 893–905 (1969).
[95]F. Yamamizu, H. Takahashi, N. Goto, Y. Ohta, and K. Shiono, "Vertical Distribution of the Seismic S-Wave Velocities at the Site of the Iwatsuki Deep Borehole Observatory of Crustal Activities," preprint of oral presentation (1976).
[96]G. Dickinson, "Geological Aspects of Abnormal Reservoir Pressures in Gulf Coast Louisiana," Am. Assoc. Pet. Geol. Bull. **37**, 410–432 (1953).
[97]H. H. Rieke, III, and G. V. Chilingarian, *Compaction of Argillaceous Sediments* (Elsevier, New York, 1974).